ELSEVIER

Valorization of wood biomass-lignin *via* selective bond scission: A minireview

Sarifuddin Gazi

Department of Chemistry, School of Applied Sciences, University of Science and Technology, Meghalaya, Techno City, Kling Road, Baridua 9th Mile, Ri-Bhoi, 793101 Meghalaya, India

ABSTRACT

Non-food biomass are examined for the production of fuel and chemicals, since petroleum is becoming less accessible. Among wood biomasses, the most underutilized component-lignin with highly crosslinked and randomly polymerized aromatic ether units becomes robust and recalcitrant to current chemical processing. Increased attentions to develop catalytic methods for lignin depolymerization are observed recently, as lignin can be the largest natural source of aromatics. The existing technologies of drastic reaction conditions do nonselective random bond cleavage yielding large variety of small molecules with less yields. Recently, selective bond scission (C−C or C−O) *via* catalytic thermal and photochemical routes have been discovered which include hydrogenolysis by transition metal complexes, metals on different supports, bimetallic catalysts with synergistic effect; bond activation with photoredox catalysts, *etc.* This mini review discusses recent progress in selective bond scission techniques with homogeneous and heterogeneous catalytic systems for the final goal of lignin valorization to value-added products.

1. Introduction

Lignocellulose consists of three distinctly different fractions, namely hemicellulose, cellulose and lignin representing more than 90% of all plant biomass and is the main renewable carbon source without competing with food reserves (Fig. 1). [1] The Hemi-cellulose is mainly polysaccharides of C_5 and C_6 units [2] comprising the biopolymer with important applications in the production of biofuel (*e.g.* bioethanol) as well as valuable chemical intermediates (*e.g.* furfural) [3]. The cellulose is comparably considered to be one of the most abundant biopolymers on our planet having linear β (1–4) glucose chain links. Cellulose can also be disintegrated into valuable products such as biofuels (*e.g.* bioethanol) and other aliphatic compounds (including small carboxylic acids, *e.g.* formic acid, lactic acid, gammavalerolactone and derived products) [4]. The third component lignin accounts for 20–35% of the weight of lignocellulosic biomass. It is a recalcitrant and complex phenolic macromolecule comprising three phenyl propanols (cinnamyl alcohols), namely, coniferyl alcohol, p-coumaryl alcohol, and sinapyl alcohol [5,6].

These three alcoholic compounds get assembled into a complex three-dimensional structure *via* different linkages. Based on the distribution of these alcoholic moieties, lignin is classified as softwood and hardwood lignin. The composition of softwood and hardwood lignin varies in the relative abundance of the *p*-coumaryl, coniferyl, and sinapyl alcohols as shown in Fig. 2. Coniferyl alcohols constitute approximately 90% of softwood lignin, whereas roughly equal proportions of coniferyl alcohol and sinapyl alcohol appear in hardwood lignin, although there are a few exceptions reported. [8] Lignin with its highly irregular crossed linked polymeric structure is accountable for the strength and shape of plants [9]. And it being internally extremely robust, is resistant to microbial attack and can prevent water from destroying the polysaccharide protein matrix of plant cells [10]. Among the constituents of lignocellulose, lignin remains as the most underutilized fraction and it has been traditionally employed as the source of heat and power through combustion in the pulp and paper industry due to its high calorific value [11]. Lignin has drawn more attention of the scientific community in the last few years since it has the polymeric structure with aromatic units connected to each other with different linkages *e.g.* β−O−4 (most dominant linkage), β-β, β-1, 4-O-5 *etc.* as shown in Fig. 2.

Thus the lignin is considered as the largest source of aromatic compounds, and therefore, the advancement in its valorization process has become a popular topic of research. [12] However, with the rigid, irregular, and highly cross-linked structure lignin showed a significant challenge for its effective degradation even with considerable efforts [13]. Lignin is generally isolated from wood during the wood pulping by three industrial processes, namely, the Kraft process, sulfite process, and the organosolv processes [14–16].These conventional methods of
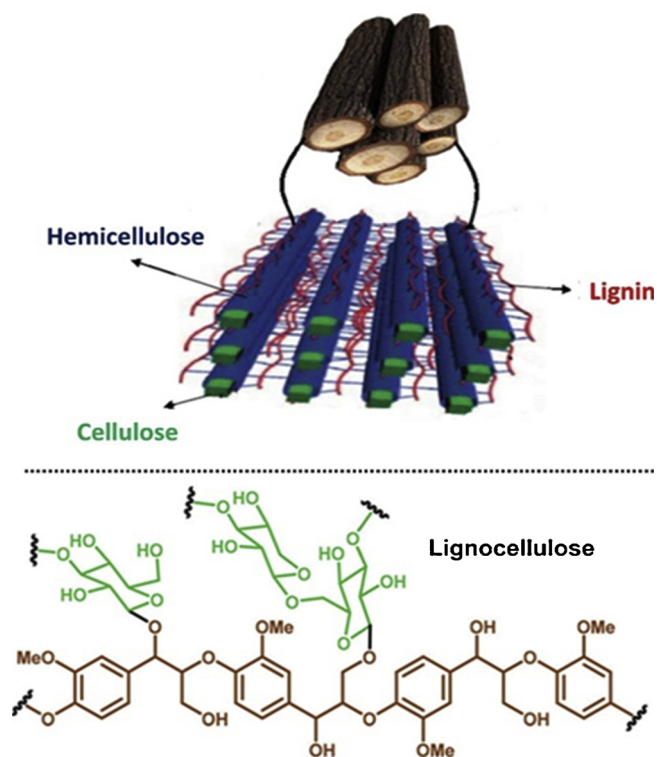
Fig. 1. Schematic representation of the locations of cellulose, hemicellulose, and lignin in plant wood cell (up). [7] And general structural representation of lignocellulose (down).

fractionation of lignocellulose, usually make structural changes in the lignin, generally leading to the form of more C—C linkages due to condensation reaction at the expense of β—O—4 bonds, making the extracted lignin less reactive and more difficult to be transformed [17]. The present industrial degradation processes of lignin use excessive chemical reagents, catalysts under high thermal environment and microbial reactions that abolish the bulk of the valuable aromatic moieties and functional groups in lignin. For example, the harsh pyrolytic and solvo-thermal processes with excessive acids or bases for hydrolysis, and hydrogen gas with metal based catalysts for reductive degradation result unselective random decomposition yielding numerous products of very low concentrations along with the competitive side reactions like mineralization and charring. [18] There are three potential strategies (Fig. 3) for biomass valorization as according to Gallezot [19] as shown in Fig. 3.

The first strategy involves the gasification of biomass to synthesis gas (CO & H_2) or degradation by pyrolysis to a mixture of small molecules, which can be used to produce chemicals using technology developed or petroleum feedstocks. [19] The second strategy includes the extensive removal of the functional groups present on the lignin monomers yielding simple aromatic compounds such as benzene, toluene, xylene, phenol *etc.* These platform chemicals are then processed under second step where the existing catalytic technology is utilized to produce bulk and fine chemicals. In the third strategy, the lignin biomass is targeted to be converted directly to valuable functionalized aromatic compounds in high yields *via* one-pot fashion, which needs highly selective catalysts that break specified functionalities and linkages. The development of the more appropriate chemical methodology for the conversion of lignin that preserves the aromatic structure while yielding value-added compounds is the most essential objective. Therefore, very recently, the major focus for the degradation of lignin has been found to be directed towards the selective C—O or C—C bond cleavage under thermal as well as photochemical routes with the help of smart catalysts which do not destroy the aromatic units and other

important functionalities. [20–25]

The various strategies applied for the depolymerization of lignin models and the native lignin *via* the selective C—O or C—C bond scission till so far can be categorized into three groups, as the reductive, oxidative, and redox-neutral bond cleavage under catalytic routes. The general routes for the selective bond cleavage (C—O and C—C) of the lignin models are depicted in the Fig. 4. These different processes will be discussed throughout this review article.

2. Selective C—O bond cleavage

In recent times, the homogeneous transition metal based complexes and heterogeneous metallic surface on solid base (carbon, metal oxides, zeolite, *etc.*) as well as metallic alloy have been utilized as catalysts for the selective hydrogenolysis of model lignin substrates under thermal conditions which generally activate the most abundant polar $C_β$–O bond of the lignin. Selective $C_β$–O bond activation under milder reaction conditions are also achieved in two steps. Here, the initial step is a selective oxidation of benzylic alcohol functionality to the corresponding carbonyl group, as a result of which the bond energy of the polar $C_β$–O bond decreases.

2.1. Selective C—O bond scission with homogeneous Ni complex

The initiation and the progress of C—O bond scission chemistry is based on the fundamental mechanistic understanding of the traditional transition metal-catalyzed cross-coupling reactions. [26–29] The application of the cross coupling reaction for the selective C—O bond cleavage involves the activation of the aryl C—O bonds by a Pd or Ni catalyst followed by the efficient transmetallating hydride transfer reaction. In this strategy, a variety of metal complexes and hydride sources have been reported for the reductive cleavage of aromatic ether linkage (sp^2C—O bonds) in lignin models. [30–32] The first report on oxidative insertion of Ni to the aryl C—O bond was made by Wenkert and co-workers in 1979 while using $NiCl_2(PCy_3)_2$ as a precatalyst to demonstrate the Ni catalyzed Kumada cross-coupling reaction in the presence of phenylmagnesium bromide (Table 1). [33] A variety of methoxy anisole and napthelene substrates were used and found to be competent substrates for the oxidative addition to Ni. Further, the methoxy napthelene substrates were found to be more reactive over the anisole derivatives as indicated by product yields. This result implied an initial occurrence of the π-coordination of the Ni^{II} complex to the substrate prior to the C—O insertion, in which the polycyclic aromatic structure of the methoxynaphthalenes, compared to the methoxybenzenes, was more docile for reactivity. The accomplishment of this protocol was an early example of a selective activation of the aryl—C—O bond over the alkyl—C—O bond by Ni-catalyst. Latter, Dankwardt *et al.* explored the Kumada cross-coupling reaction with increased substrate scope by employing a more electron-rich Ni catalyst. [34]

After initial report by Wenkert and co-worker, Ni-aided C—O bond activation to C—C bond formation strategies have been explored for a large variety of the oxyarene bonds including carbamates, carbonates, mesylates, vinyl esters, sulfonates, sulfates *etc.* [35–37] A major breakthrough research finding was observed by Martin and co-workers while treating the aryl ether substrates using Ni-complex with hydride transferring reagents.

Martin's approach under the optimal reaction condition, demonstrates a homogeneous cross-coupling method in which hydride transmetalation followed by the reductive elimination reaction yields a deoxygenated arene (Scheme 1). [38]

After Martin's finding, Hartwig and Sergeev reported their extensive research on the reductive aryl—C—O bond cleavage of a variety of alkyl-aryl ether substrates including the lignin model compounds using Ni–NHC (N-heterocyclic carbene, SIPr) complex. Practically, Hartwig and his team established a general substrate tolerance of Ar–OAr, Ar–OMe, and $ArCH_2$–OMe, showcasing the ability of Ni-NHC to reduce
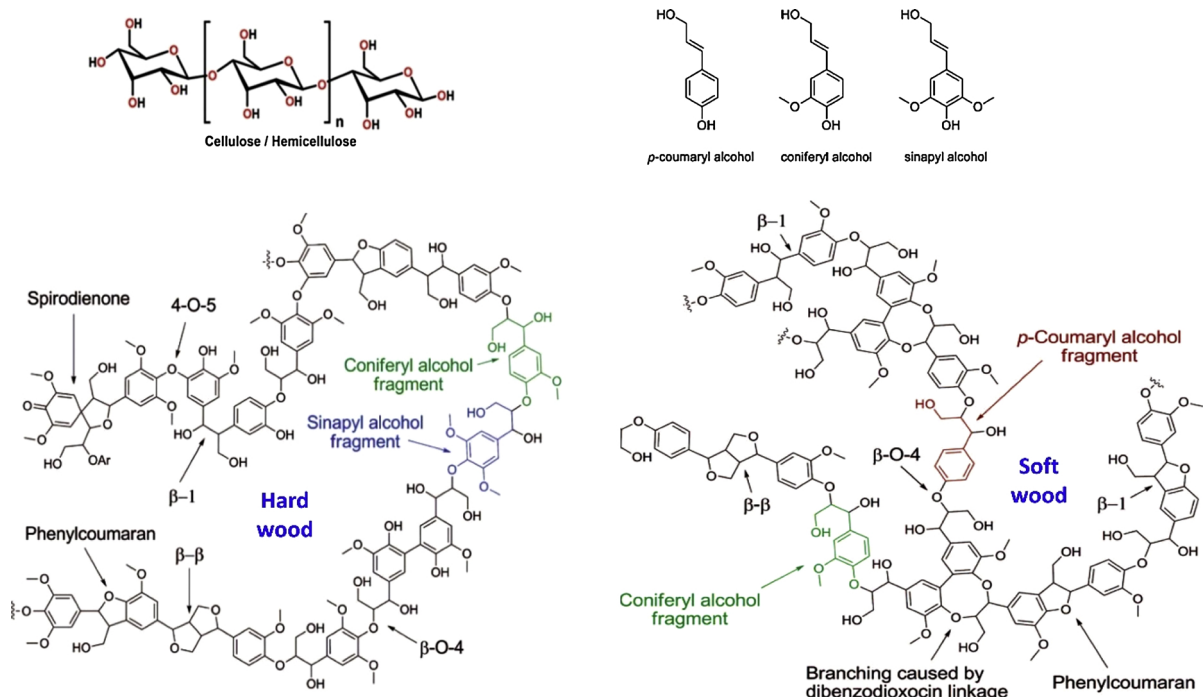
Fig. 2. Structural presentation of cellulose/hemicellulose, hard and softwood lignin with their different alcoholic constituents. [10] Reprinted with permission from Ref. [10]. Copyright 2010 American Chemical Society (Chemical Reviews).
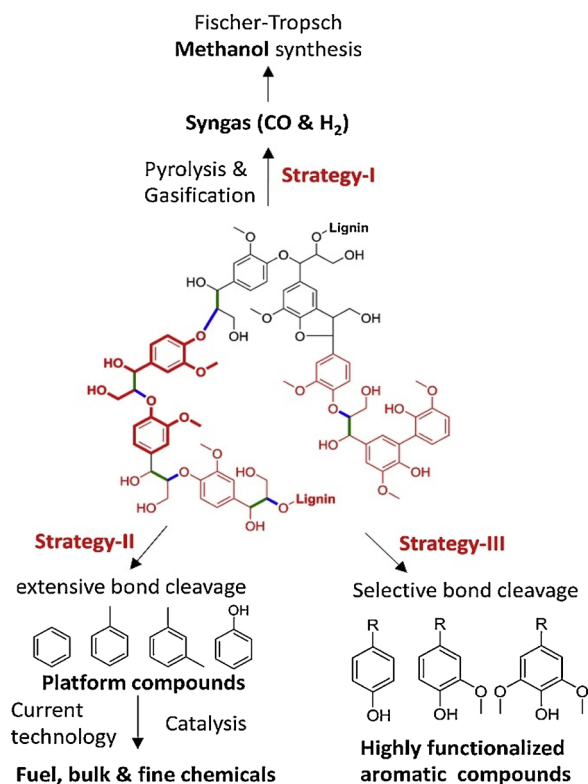

Fig. 3. Different strategies for the valorization of the wood biomass-lignin.

both sp^2C—O and sp^3C—O bonds in the presence of molecular hydrogen gas.

Interestingly, Ni–NHC catalyst (Fig. 5) used in their studies can selectively reduce aryl–aryl ethers in the presence of aryl–alkyl ethers that shows the possibility for the 4-O-5 disintegration selectively of lignin models (Table 2). [39]

Hartwig and his team observed that the Ni(COD)$_2$ complex in the presence of NHC ligand SIPr.HCl behaves differently with different ether substrates (Fig. 5). The same group has successfully exemplified the reactivity of the Ni(COD)$_2$ complex in the presence of NHC ligand SIPr.HCl on different substrates having distinct ether linkages, for examples macro molecule with Ar—OAr linkage, compounds with 4—O—5 linkage, α—O—4 linkage and also β—O—4 linkage towards the reductive C—O bond cleavage as shown in the scheme 2 [39].

In spite of the high selectivity and mild reaction conditions in comparison to the classical hydrogenolysis reactions of lignin, Hartwig methodology needs high loadings of potassium tert-butoxide as an additive and an expensive NHC ligand. However, Hartwig and co-workers latter reported the reductive C—O bond cleavage reaction methodology under the ligand (NHC ligand) free heterogeneous reaction condition where the catalyst is reported to be formed *in situ* from the soluble nickel precursor complex Ni(CH$_2$TMS)$_2$(TMEDA) or Ni(COD)$_2$ in the presence of a base additive, such as ^{t}BuONa. [40] Interestingly, they observed that the reactivity of the Ni-complex in the presence of NHC ligand towards the C—O bond cleavage increases with the increase in electron density of the aryl ethers (Fig. 6). And for the ligandless Ni-complex, the reactivity of the *in situ* generated heterogeneous Ni-system the opposite trend was observed (Fig. 6).

2.2. Selective C—O bond scission with V complex

Sunghee Son and F. Dean Toste recently in 2010 have reported a highly selective oxovanadium complex as the catalyst which can cleave the C—O bond of β—O—4 lignin models under the aerial condition with an elevated temperature. [41] Interestingly, this methodology does not need of any other additives (Scheme 3). [41] In their study, the Son *el al.* has found that towards the C—O bond cleavage reaction, the oxovanadium complexes behave differently in comparison with the previously reported Hartwig's degradation conditions where sp^2C—O cleavage is more preferable over the sp^3C—O cleavage.

To get a most selective catalyst for C—O bond cleavage of the β—O—4 lignin linkage, Son *el al.* has screened a number of different oxovanadium complexes as shown in the Fig. 7. Based on the distribution of the products for different lignin models and the

A. Selective C–O Bond Cleavage

I. Selective sp³C_β–O Bond Cleavage: Benzylic-H abstraction
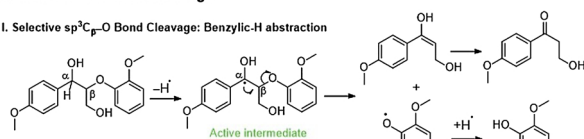
II. Selective sp³C_β–O Bond Cleavage: Photoredox reduction
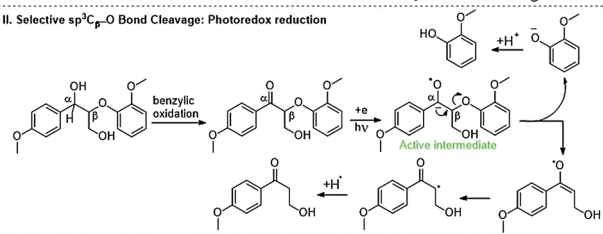
III. Selective sp³C_β–O Bond Cleavage: Transfer hydrogenolysis
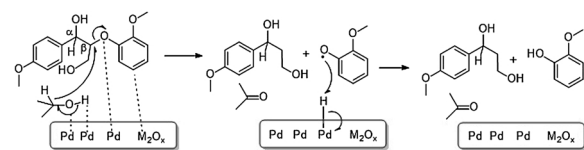
B. Selective C–C Bond Cleavage

I. Selective sp³C_α–C_aryl Bond Cleavage: H-abstraction to phenoxy radical
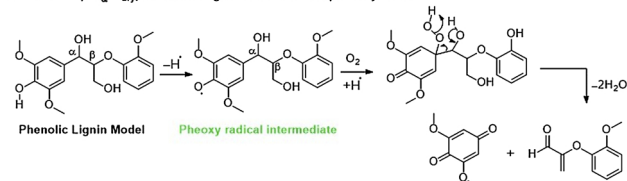
II. Selective sp³(C_α–C_β) Bond Cleavage: LMCT to reactive intermediate
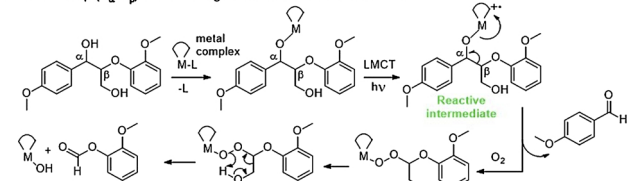
III. Selective sp³(C_α–C_β) Bond Cleavage: H-abstraction to alkyl radical
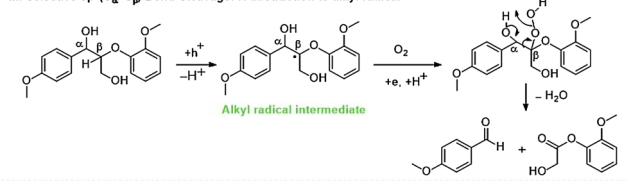
Fig. 4. (A) Some important routes of selective C–O bond scission of lignin models *via* benzylic H-abstraction [23], benzylic alcohol oxidation followed by photoredox reduction [24], and transfer hydrogenolysis [25]. (**B**) Some important routes of selective C–C bond scission of lignin models *via* H-abstraction to phenoxy radical [23], ligand to metal charge transfer (LMCT) driven photoredox C–C bond activation [24], and H-abstraction to alkyl radical generation [24].

spectroscopic analysis, the group has proposed a one-electron process as the most plausible mechanism (Scheme 4). In the mechanistic route according to them, after ligand exchange on the vanadium complex with the benzylic hydroxyl group, the benzylic hydrogen is abstracted to generate the ketyl radical which helps in eliminating the aryloxy radical. The hydroxy group after being eliminated from the resulting enolate produces α-β unsaturated ketone and a vanadium (IV) complex, which gets re-oxidized to vanadium (V) by the aryloxy radical.

Toste et al. conducted also the selective C–O bond scission of the trimeric lignin model having β–O–4 linkage (Scheme 5). Interestingly, in this case also the most active oxovanadium catalyst showed its high

Table 1
Aryl C–O bond activation followed by sp²C–sp²C bond formation with Ni complex.

Substrates	Products	Yields (%)
		20
		33
		23
		77
		45

Scheme 1. C–O bond reduction of aryl ethers by Ni-catalyst in the presence of TMSDO (TMSDO = 1,1,3,3-tetramethyldisiloxane).

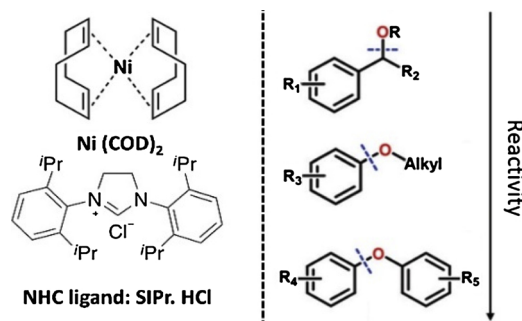**Fig. 5.** Structures of the NHC ligand, the Ni(COD)₂ complex and their reactivity order towards different ether compounds.

selectivity property, confirmed by the distribution of the degradation products. Latter, the same group has extended their investigation of this oxovanadium catalysis towards the actual lignin degradation study. [42]

They have isolated the organosolv lignin from *Miscanthus giganteus*, treated with their most active oxovanadium complex and successfully got the monomeric value added compounds (Table 3). [42]

Table 2
Hydrogenolysis of diaryl ethers using 1 bar of H_2 gas leading to the reductive cleavage of the C—O bond.

Substrates	Time (h)	Arene (%)	Phenol (%)
	16	(99)	(99)
	16	(96)	(99)
	16	(86)	(88)
	48	(97)	(99)
	48	(72)	(73)
	16	(87)	(99)
	16	(87)	(92)
	16	(88)	(80)
	32	(85)	(85)

2.3. Selective C—O bond scission with heterogeneous Pd/C

Demonstration of C—O bond cleavage of the β—O—4 lignin model systems using Pd/C and transfer hydrogenation reaction was done by Samec and co-workers (Scheme 6). [43] These conditions were developed by screening a variety of transition metals and hydrogen donors. A comparative study of Pd/C, Rh/C, Ir/C, Re/C, Ni/C, revealed that Pd was unique in reducing the β—O—4 model compounds to the corresponding phenol and acetophenone.

Selectivity of the β—O—4 cleavage reaction was enhanced by the addition of a stoichiometric equivalent of amine (ammonia, ethyl amine, allylamine). Also the presence of formic acid was found to efficiently facilitate reduction as compared to H_2 or 2-propanol.

2.4. Selective C—O bond scission with heterogeneous Pt/C

Again, according to Yan et al. noble metal catalysts have revealed high selectivity for C_β—O bond cleavage to yield aromatic monomers. [44] Similarly, Kim et al. have reported that Pt/C was the most effective catalyst in the depolymerization of lignin in comparison to Pd/C, Ru/C, and Ni/C catalysts. The same group reported that when Pt/C has been used as catalyst for disintegration of lignin *via* hydrogenolysis, it yielded large amounts of lignin-oil (77.4 wt%) with the smallest amount of char (3.7 wt%), as well as 4-ethylphenol, guaiacol, 4-ethylguaiacol, and syringol as the monomeric phenolic products. [45] The use of noble metal catalysts for the biomass degradation process are not encouraged as the catalysts are expensive; to make the process more cost effective,

supporting materials are utilized for the dispersion of the metal and also to control the size of the metal clusters. Therefore, the primary focusses of the research on Pt catalysts are found to be targeted on finding optimum supporting materials. Carbon is reported as an exceptional support for Pt. But, if carbon can be synthesized with well-regulated pore structure for increasing the dispersion of the catalyst, the integrated composition will be expected to act as an effective catalyst for lignin depolymerization [46]. Keeping this concept in mind Park et al. investigated the degradation of lignin and reported their findings on the correlations between the surface area of the catalyst and the characteristics of the depolymerized lignin products. They prepared three different supports (mesoporous carbon (STC), porous carbon (TC), and microporous carbon (DC)) and impregnated Pt on those and tried to find out their activities on lignin depolymerization. They considered 5 wt% Pt on commercial activated carbon (Pt/C) for comparative study too. Surface area of the catalysts was reported in the order of Pt/C (1506.49 m^2 g-cat.$^{-1}$) > Pt/STC (832.62 m^2 g-cat.$^{-1}$) > Pt/TC (490.93 m^2 g-cat.$^{-1}$) > Pt/DC (374.35 m^2 g-cat.$^{-1}$). Yields of the monomeric phenols (90.92, 78.06, 64.33, 53.22 mg. g^{-1} of lignin, respectively) were found to follow the same trend as the BET surface area of the catalysts. [47]

2.5. Selective C—O bond scission with bifunctional heterogeneous metal catalysts

The research works to find out the alternatives to the catalysts based on noble metals are found to be prominent in recent literatures. A few
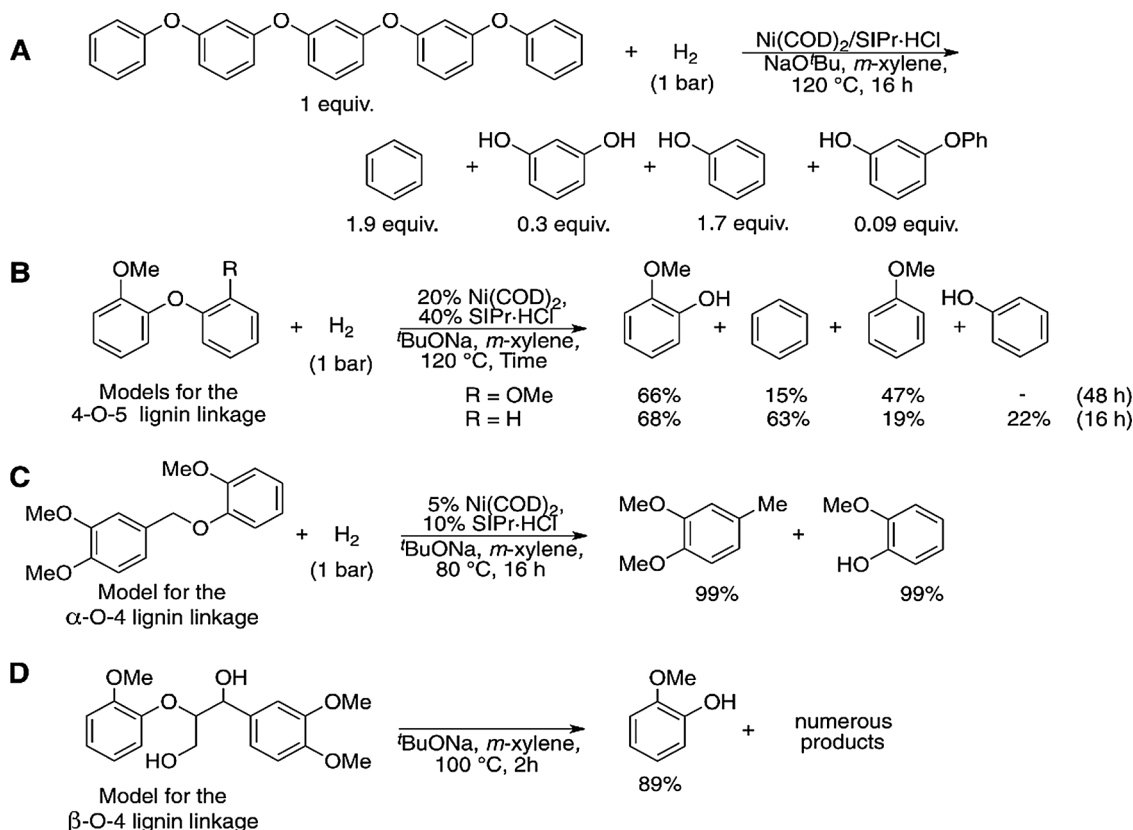
Scheme 2. Hydrogenolysis of (**A**) compound bis(m-phenoxyphenyl)benzene. (**B**) A lignin model compound having 4−O−5 linkage. (**C**) A lignin model compound of α−O−4 linkage. (**D**) A lignin model compound having the β−O−4 linkage. [39] Reprinted with permission from Ref. [39]. Copyright 2011 Science.
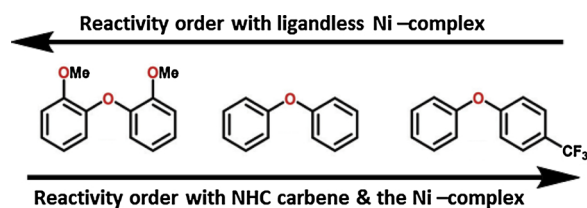

Fig. 6. Orthogonal relation of reactivity of Ni complex with and without NHC ligand.

interesting reports are found based on niobium catalysts. Although in catalysis industries, niobium compounds are not widely implemented, there are evolving results describing the catalytic activities of niobium compounds. [48–51] The niobium-based catalysts are found to have high stability and hence in biomass valorization, they can be used for several cycles in batch reactors or for hundreds of hours in fixed-bed reactors. Again, niobium can be recovered from the deactivated catalysts by treating it with hydrofluoric acid [52]. Shao and co-worker have presented a Ru/Nb$_2$O$_5$ catalytic process for one-pot valorization of raw lignin to hydrocarbons. [53] They achieved high mass yields and selectivities. Phenolic products are reported to be formed by the
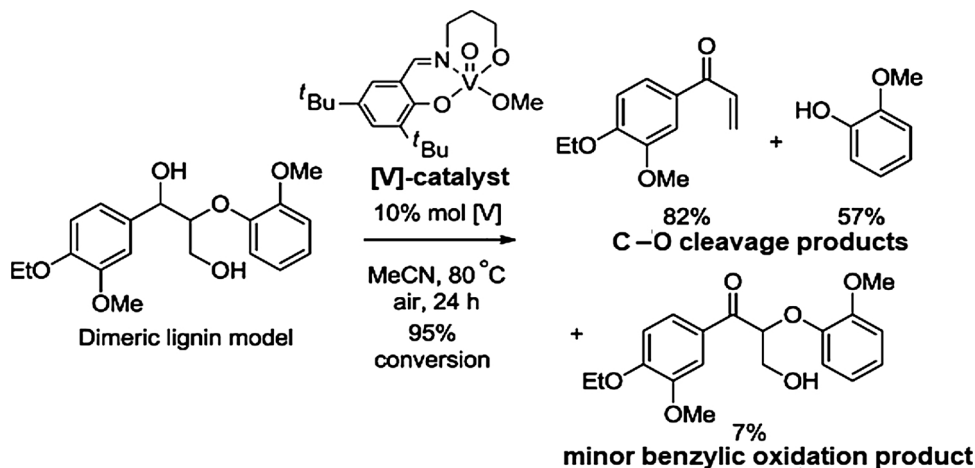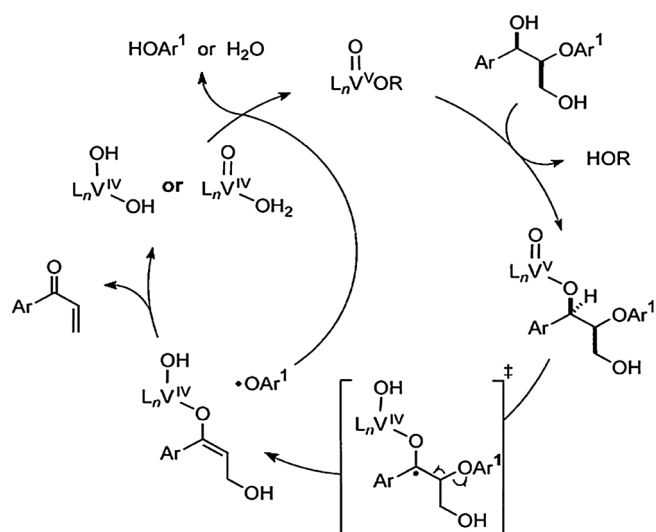

Scheme 3. Products *via* C–O scission and benzylic oxidation by vanadium catalyst.
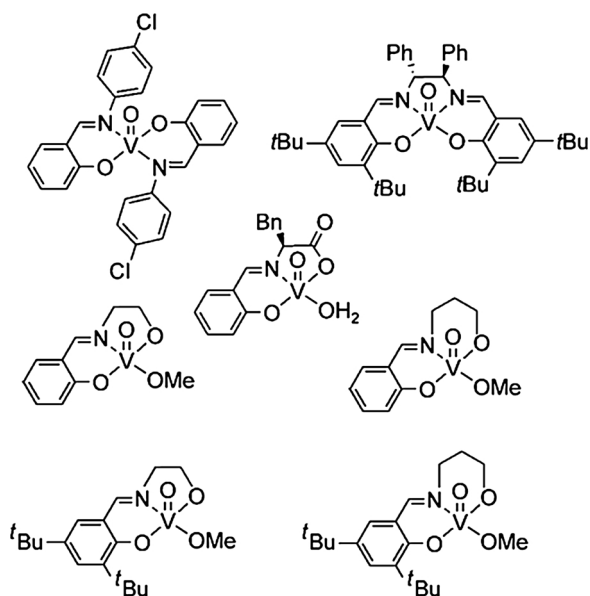
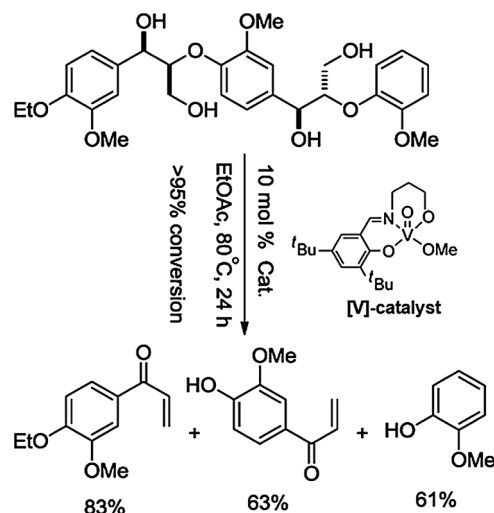**Fig. 7.** Various oxovanadium complexes screened by Son et al. for selective C−O bond cleavage of β−O−4 lignin linkage.

Scheme 5. Degradation of a trimeric lignin model by the oxovanadium catalyst.

Scheme 4. Plausible mechanism for the vanadium-catalyzed non-oxidative cleavage of the β−O−4 lignin linkage. [41] Reprinted with permission from Ref. [41]. Copyright 2010 Angew. Chem., Int. Ed.

Table 3
Compounds formed *via* vanadium-catalyzed degradation of dioxasolv-lignin (1.0 mg 0.50 ml of solvent) and were identified by GC/MS study [42].

Entry	Degradation product	Quantity formed (μg)
1	Vanillin	7.8
2	syringic acid	6.7
3	syringaldehyde	5.9
4	4-hydroxybenzaldehyde	3.3
5	Vanillic acid	3.1
6	3-hydroxy-1-(4-hydroxy-3-methoxy phenyl)propan-1-one	1.2
7	3-hydroxy-1-(4-hydroxy-3,5-dimethoxy-phenyl)propan-1-one	0.8
8	4-hydroxybenzoic acid	0.5

cleavage of C_β–O bonds in lignin by this hydrodeoxygenation reaction, which further underwent hydrogenolysis to yield arenes. Degradation studies on model compound revealed that phenols were transformed into aromatic hydrocarbons through the selective scission of C_{aryl}−OH bonds over the Ru/Nb$_2$O$_5$ catalyst, under high temperature. The high reactivity of Nb$_2$O$_5$ support is optimized in comparison with alumina, titania, and zirconia. This one-pot approach offers an energy-efficient, simpler technique for the valorization of lignin into value-added arene feedstocks. [53]

The state-of-the-art petroleum refineries mainly utilize zeolite-based catalysts for hydrocarbon cracking and pyrolysis to produce small-molecule feedstocks. [54] But recently, a catalytic system, Ru/NbOPO$_4$ has been reported to be superior than that of conventional zeolite-based catalysts. [55] This catalytic system offers one-pot conversion of lignin by cleaving of both interunit C–C and C–O efficiently, and also effectively prevents the deep C–C cracking of low-molecular-weight
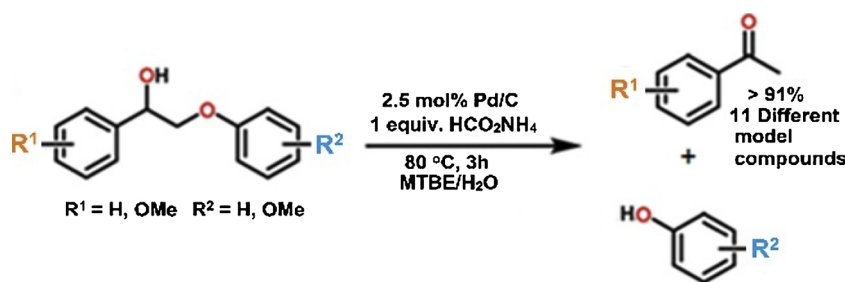
Scheme 6. Pd-catalyzed C−O bond cleavage of β−O−4 lignin model systems at elevated temperature.

products. Thus, under mild conditions, the catalytic system yields in the isolation of desirable liquid C_6–C_9 monocyclic hydrocarbons. [55]

A seminal report on Au/Nb_2O_5 catalytic system has been found also for the highly selective conversion of lignin to phenolic compounds with high yields. [56] Unlike previous catalytic systems, this approach avoids the hydrogenolysis of phenolic hydroxyl groups and reduction of aromatic rings. Similar studies with model compound revealed that 2-methoxy-4-propylphenol was firstly converted into propylcatechol, which further underwent hydrogenolysis to yield propylphenol. The superior activity of the Au/Nb_2O_5 catalyst for lignin valorization is due to the following three facts: 1) the strong acidic sites present on the support, Nb_2O_5 catalyze the hydrolysis reaction; 2) the negatively charged Au species help in the dissociation of H_2 significantly during the hydrodeoxygenation; and 3) the NbO_x species assist in cleaving the C_{aryl}–OH bond. Additionally, water medium increases the selectivity to the phenolic products by preventing transmethylation reaction completely. [56] This one-pot catalytic process offers a more efficient technique for selective conversion of lignin biomass into value-added phenolic products in comparison with complete deoxygenation.

2.6. Selective C−O bond scission with other heterogeneous metal catalysts

Again, there are a number of Raney nickel catalysts [57] found in the literature for the hydrocracking of organosolv lignin in subcritical water where the yields of phenols are reported to be 1.3–8.0%. The stability of the catalysts and their poor activity have limited their applications in lignin depolymerization [58–63]. The possibility to enhance the selectivity and yield of degradation products may be there by using bimetallic catalysts [64] which is due to a phenomenon called 'synergistic effects'. [65–69]Therefore, bimetallic catalysts based on nickel have been reported for depolymerizing lignin. S-Co-Mo/MgO-La_2O_3 has been utilized for catalytic hydrotreatment of the Kraft lignin and which yielded 26.4% of monomeric products at 350 °C, 10 MPa hydrogen. [70] Whereas the catalytic system S-Ni-W/AC resulted an improved yields (28.5%) of monomers at 320 °C, 3.5 MPa hydrogen [71]. The bimetallic catalysts Ni-Au and Ni-M (M = Ru, Rh and Pt) showed good selectivity for β−O−4 ether linkages hydrogenolysis, but the yield of monomer was reported to be less (6.8%) when organosolv lignin has been used [72,73]. The use of ZrO_2 supported Pd-Ni bimetallic catalyst was reported for efficient and selective hydrogenolysis of β−O−4 linkages in lignin model compounds. [74] There is another report which revealed that Fe can stimulate the deoxygenation of lignin in the presence of Ni/SiO_2 [75]. Again, $FeCl_3$ has also been utilized as a co-catalyst with Pd/C to depolymerize lignin. [76] The higher hydrodeoxygenation selectivity without over-hydrogenation of aromatic rings was found with Fe/C catalytic system [77]. Based on these previous studies, recently, non-precious bimetallic Ni-Fe/AC catalysts have been developed to gain better selectivity with higher yields of monomers from lignin degradation reaction under relatively mild reaction condition [78]. The experimental results revealed that the catalyst with 1:1 ratio of Ni and Fe exhibited the highest catalytic activity without hydrogenation of benzene ring. Here, in this study the total yield of monomers from birch lignin was reported as 39.5%. This non-precious

metallic Ni-Fe/AC catalyst exhibited very good activity in the production of monomers *via* lignin depolymerization. [78]

2.7. Oxidatively selective C−O bond scission in ionic liquids

In the literature a significant number of papers have been found focusing on the selective cleavage of the β−O−4 linkages in lignin, as well as its oxidative degradation in ionic liquids. Hallett et al. investigated the structural changes occurred in the Miscanthus giganteus lignin after extraction with 1-butylimidazolium hydrogen sulfate ([HC$_4$im][HSO$_4$]), a protic ionic liquid. [79] The spectroscopic and elemental analytical results suggested that the lignin was decomposed *via* β−O−4 bonds cleavage. The molecular weight of lignin was reported to be decreased from M_w = 12,400 g/mol to M_w = 6770 g/mol in this process. Here, the preliminary analysis suggested the formation of monomeric phenolic compounds like syringols, guaiacols and phenols along with some sugar degradation products. Similarly, An et al. studied the dissolution of kraft lignin in cholinium ionic liquids. [80] Here also, the experimental results revealed that the β−O−4 linkages in kraft lignin were broken. Sun et al. also investigated the chemical transformations of lignin by the ionic liquid treatment [81]. This work described the effect of 1-ethyl-3-methylimidazolium acetate ([C$_2$mim] [OAc]) treatment with variation of the reaction temperatures and reaction times on structure of lignin. The results yielded the scission of β−O−4 linkages, along with β-β' and β-5' bonds. Consequently there was a decrease in molecular weight observed. Again, Fu et al. established a pathway of oxidatively depolymerization of eucalyptus kraft lignin in 1-butyl-3-methylimidazolium chloride ([BMIM]Cl) with CuO as catalyst in the presence of molecular oxygen. The main products obtained in this process were vanillin, vanillic acid, syringaldehyde and syringic acid, and acedosyringone. Here, the C_α−C_β and C_β–O bonds were found to be cleaved to yield the degradation products. [82] Diop et al. showed a novel strategy to disintegrate lignin in butyl-1,8-diazabicyclo[5.4.0]undec-7-enium chloride ([DBUC$_4$][Cl]) in absence of any catalyst. Here, kraft lignin was kept in [DBUC$_4$][Cl] and the reaction was performed at different temperatures (150, 200, and 250 °C). [83] Here, also the analytical studies confirmed the occurrence of cleavage of β−O−4 bonds along with demethylation of lignin. In this process molecular weight was found to be decreased by 23, 70, and 58% at different temperature of 150, 200, and 250 °C, respectively. Oligomers were the major products under this process [83].
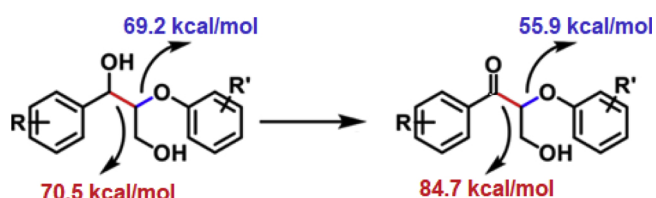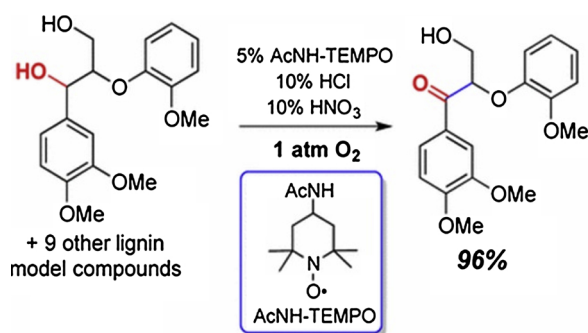

Fig. 8. The calculated BDE of the C−C and the C−O bonds in β−O−4 linkage before and after the oxidation. [84].

Scheme 7. Chemoselective oxidation of lignin model.

Scheme 9. Depolymerization of the oxidized aspen lignin.

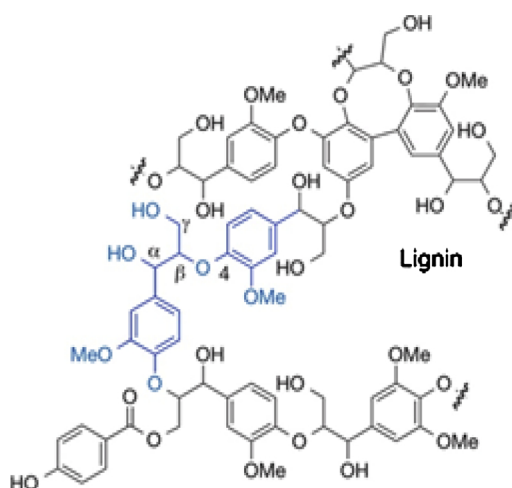## 2.8. Selective C−O bond scission via two steps

Another typical strategy to cleave the C_β–O bond in β−O−4 linkage involves two steps, where, initial oxidation of C_α−OH of β−O−4 alcohols to β−O−4 ketones followed by C_β–O bond cleavage makes the method very efficient. Theoretical studies revealed that the first oxidation of C_α−OH to C_α=O can reduce the bond dissociation energy (BDE) of C_β–O bond by 13.3 kcal/mol, which then can be easily cleaved by reduction (Fig. 8). [84]

After a rigorous screening on the oxidizing reagents, Rahimi et al. in 2013 developed and applied a chemoselective aerobic oxidation method for the oxidation of C_α alcohols to ketones for a number of lignin models (Scheme 7). [85]
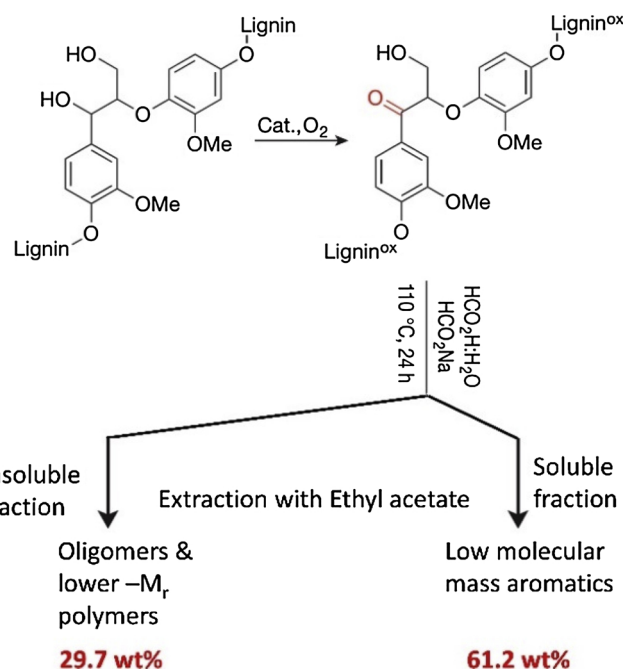
The chemoselective oxidation methodology was also examined to native lignin, which achieved, 90% conversion to oxidized lignin (Scheme 8). [85] Latter this achievement encouraged them for the direct investigation of the reactivity of oxidized lignin [86].

The oxidized lignin was treated with the formic acid and sodium formate reagent combination at the elevated temperature of 110 °C. About three equivalents of formate per S/G aromatic subunit is required as optimal reaction condition. The residue produced by evaporation of formic acid after the 24 h of reaction, was extracted with ethyl acetate. A soluble and insoluble fractions, corresponding to 61.2 wt% and 29.7 wt% of the original lignin respectively, were obtained (Scheme 9). Stahl and his team has carried out an extensive mechanistic investigation. Based on the kinetic studies and the isotope lebeling experiments they proposed the plausible reaction pathway of the selective C_β–O bond scission of the oxidized lignin model (Scheme 10).

After the report of Rahimi et al., Westwood and co-workers have documented a different reagent combination for the selective C_β–O bond cleavage of lignin model and native lignin via two steps process.

[87] Here, they employed the catalytic amount of DDQ in presence of ^tBuONO for the oxidation reaction and excess Zn/NH_4Cl for the reductive C_β–O bond cleavage of the lignin model and the birch lignin under thermal condition.

Stephenson and his team reported the photocatalytic C_β–O bond cleavage of the oxidized lignin model [88] at room temperature (Scheme 11), after the discovery of the chemoselective oxidation of C_α alcoholic functional group of the native lignin by Rahimi et al. They found that with the increase in electron density of the model substrates the reactivity towards C_β–O bond cleavage decreased.

Latter, the same group has developed a direct selective degradation methodology by merging the palladium chemistry with photoredox catalysis (Scheme 12). [89]

Non-oxidized lignin model can be directly degraded to valuable compounds via this route. [89] Very recently, the same group has developed a selective degradation methodology where the electrochemical oxidation of the C_α−OH alcohols, and the photochemical C_β–O bond cleavage reaction of lignin models and also lignin having β–O–4 linkage occur in one pot. [90] In this study the native lignin


Scheme 8. Chemoselective oxidation of native lignin.
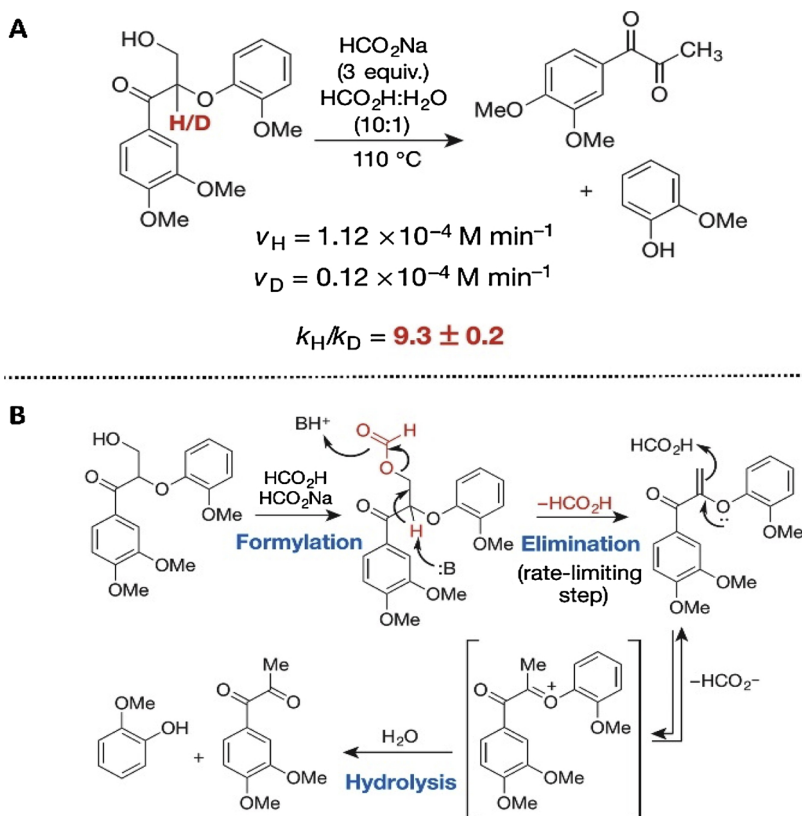
Scheme 10. (**A**) Kinetic isotope effect for cleavage of the oxidized model compound and (**B**) Proposed mechanism for C_β–O cleavage. [86] Reprinted with permission from Ref. [86]. Copyright 2007 Science.

which was isolated from pine was exposed to the one-pot reaction conditions. The isolated lignin was homogenized in a mixed solvent system, particularly in acetone/DMSO (98:2). Then this homogeneous solution of native lignin was selectively oxidized under the optimal electrocatalytic oxidation conditions. After that it was allowed for the photocatalytic cleavage reaction in the flow technique which afforded a controlled fragmentation of native lignin as supported by spectroscopic analysis. The formation of oligomeric and monomeric units with lower molecular weight (~43 wt % of oligomeric units, and up to 55 wt % of low molecular weight units) was confirmed by the gel permeation chromatographic (GPC) analysis. The product analysis revealed that there were cleavage of two consecutive β–O–4 linkages under the applied reaction conditions, which demonstrates that the developed electrocatalytic oxidation and subsequently photocatalytic cleavage is

not only highly effective in fragmenting β–O–4 bonds but also highly selective too. Here, the route of the reductive C_α–O bond cleavage is grounded on the well-established reductive quenching cycle of the photocatalyst, $[Ir(ppy)_2(dtbbpy)]PF_6$. The photocatalyst initiates a metal-to ligand charge transfer to produce the excited state $[Ir]^{3+*}$ upon visible light absorption. This excited state gets reduced to $[Ir]^{2+}$, a strong reductant (-1.51 V *vs* SCE) by taking an electron from the amine or amine–formate complex. The $[Ir]^{2+}$ complex does reduction by transferring a single electron to the benzylic ketone (pre-oxidized lignin models) to produce a corresponding radical anion, which experiences a fragmentation process to harvest an alkoxy anion and the C_α – radical. Protonation of the alkoxy anion and H-atom abstraction by C_α – radical produces the fragmentation products (phenolic and carbonyl substrates). Although the approach of Stephenson and his team
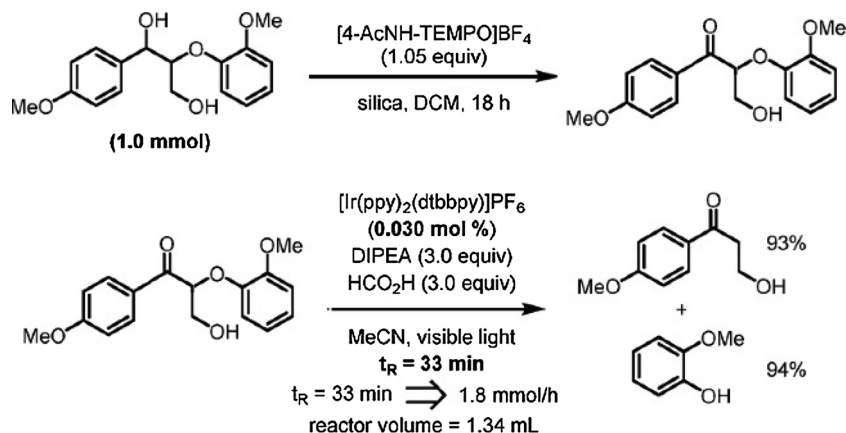
Scheme 11. Chemoselective oxidation of lignin model with slight excess of [4-AcNH-TEMPO]BF$_4$ silica and followed by selective C$_\beta$–O bond cleavage under visible light.
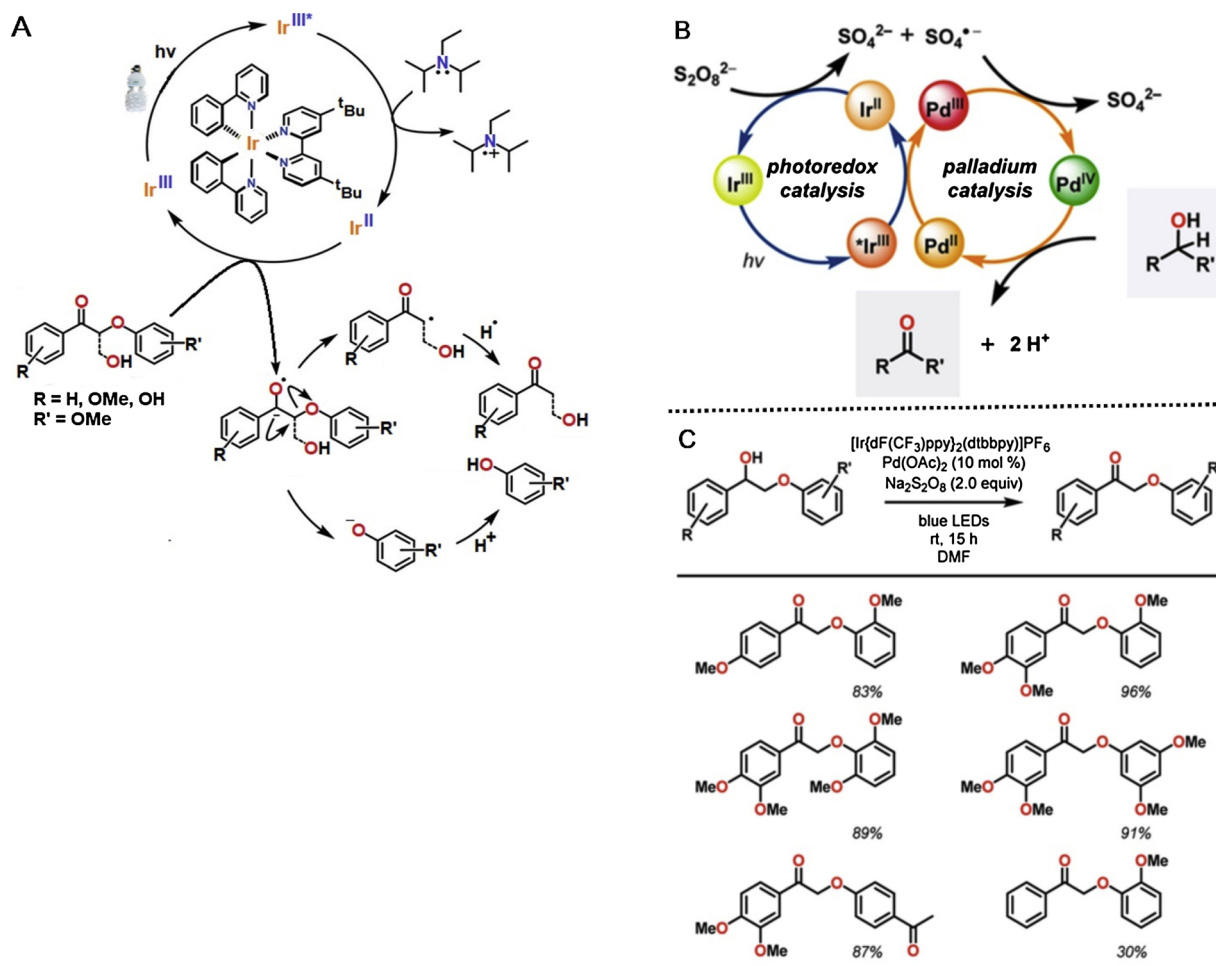
Scheme 12. (**A**) Proposed photocatalytic mechanism of C_β–O bond cleavage of oxidized lignin model, (**B**) Photocatalytic oxidation mechanism by merging palladium chemistry with photoredox catalysis, and (**C**) Scopes of the substrates. [88,89].

for the photoredox catalytic depolymerization is very efficient and most importantly, it uses milder reaction conditions, [88,90] the method needs highly expensive iridium based photocatalysts and excessive additives (DIPEA = N,N-diisopropylethylamine, and formic acid) that offers further research work for the development of more convenient methodology in the related filed. In this regard, a metal-free, visible-light active photocatalysts would be more desirable.

Zhang's research team working on developing heterogeneous photocatalysts based on carbazolic porous organic frameworks (POFs) [91,92] recently reported that metal free POFs can be the alternative to iridium photoredox catalysts for the selective C_β–O bond cleavage reaction of lignin model having β−O−4 linkage.

The research group found that under optimal condition, CzCP100/NHPI/O_2 photocatalytic system exhibited high oxidation reactivity with
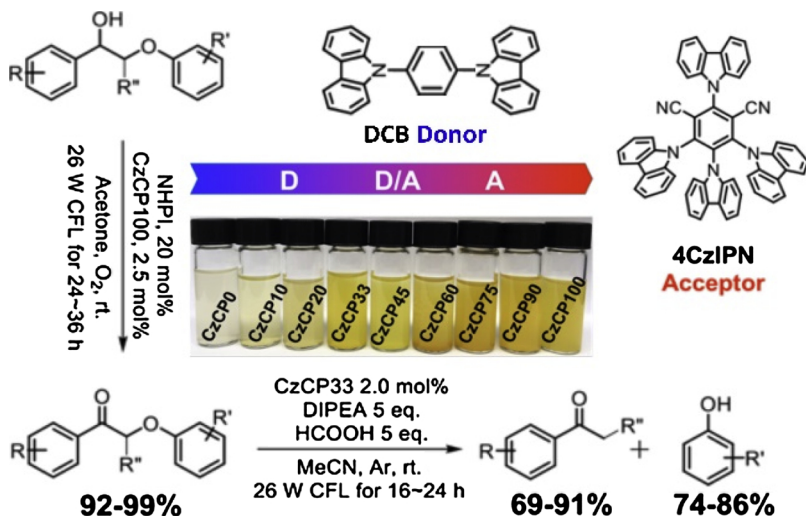
Scheme 13. Stepwise degradation of lignin β−O−4 models *via* photocatalytic C_β–O bond cleavage using carbazolic copolymers (CzCPs) as heterogeneous photoredox catalysts [where, DCB = 1,4-di(9H-carbazol-9-yl)-benzene as donor, 4CzIPN = 1,2,3,5-tetrakis (carbazol-9-yl)-4,6-dicyano-benzene as acceptor, NHPI = N-hydroxyphthalimide as hydrogen atom transfer (HAT) catalyst, CzCP33 (Donor : Acceptor = 66:33) and CzCP100 (Donor : Acceptor = 0:100)]. [93].
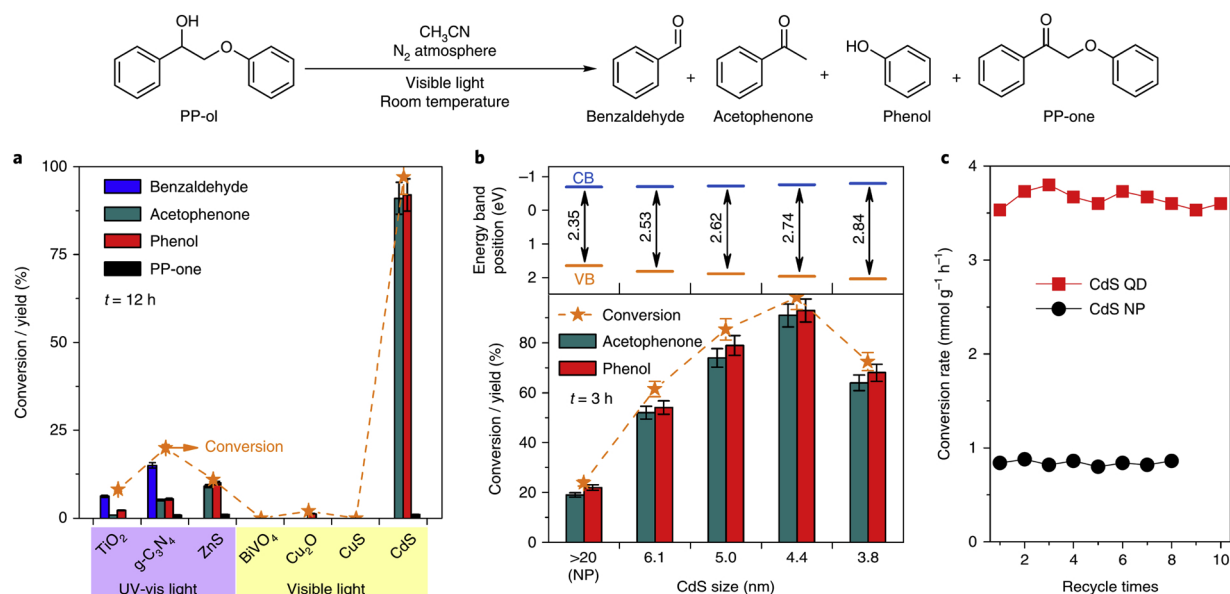
Fig. 9. Photocatalytic cleavage of **β−O−4** bond in lignin model compounds. (**a**) Photocatalytic conversion of PP-ol with several typical semiconductors. (**b**) Energy-band positions and photocatalytic performances of CdS with different sizes. (**c**) Repeated uses of CdS NPs and CdS QD −4.4 nm for the conversion of PP-ol. The reaction was carried out under visible light irradiation (λ = 420–780 nm). The UV–vis light (λ = 300–780 nm) irradiation was applied to several semiconductors in Fig. 9a. The experiments in each case were performed at least three times. The error bars represent the relative deviation, which is within 5%. The curves in each figure are guides to the eye. [94] Reprinted with permission from Ref. [94]. Copyright 2018 Nature Catalysis.
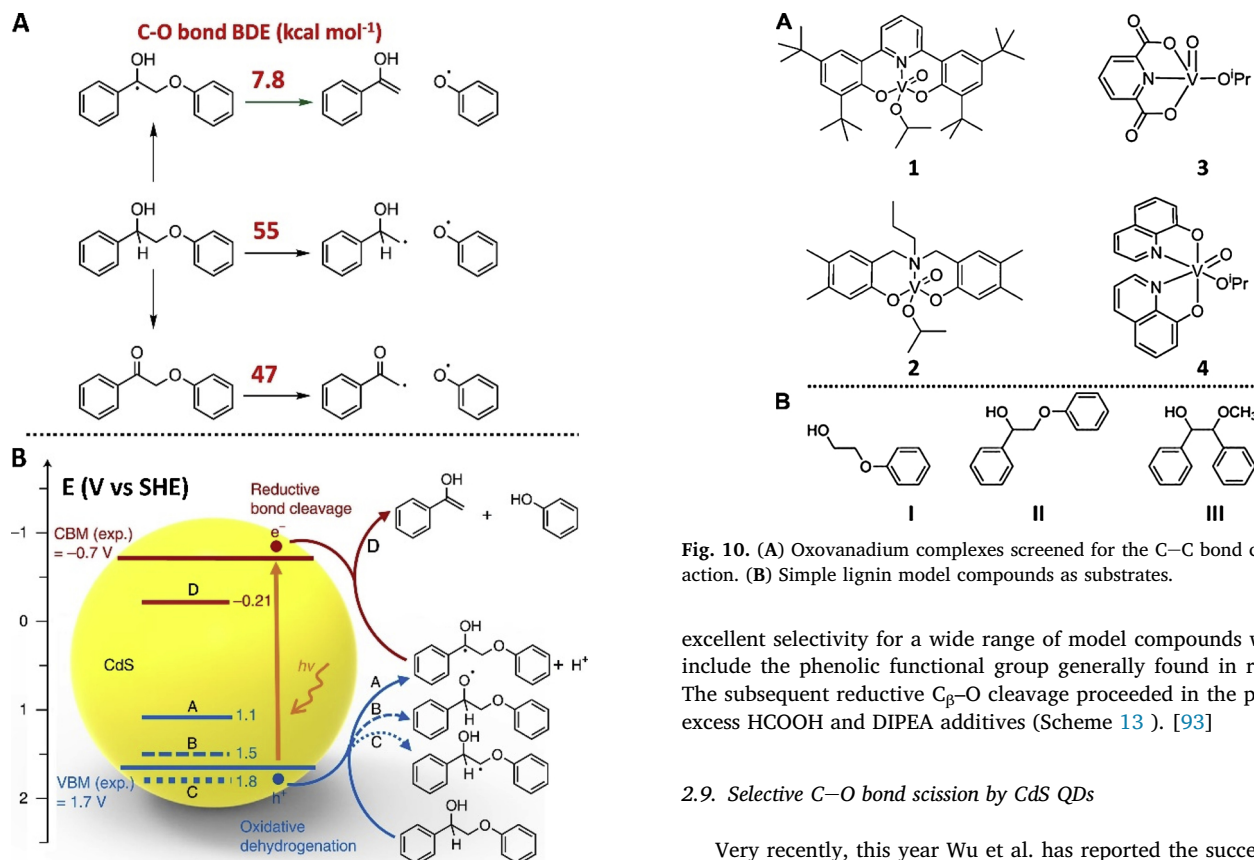
Scheme 14. (**A**) Comparison of BDE of the β−O−4 bond in C_α radical with those in alcoholic lignin model and oxidized model, (**B**) Potentials of oxidative dehydrogenation of alcoholic lignin model *via* three different paths (A, B, C) and potential of reductive cleavage of β−O−4 bond in the C_α radical intermediate. [94] Reprinted with permission from Ref. [94]. Copyright 2018 Nature Catalysis.
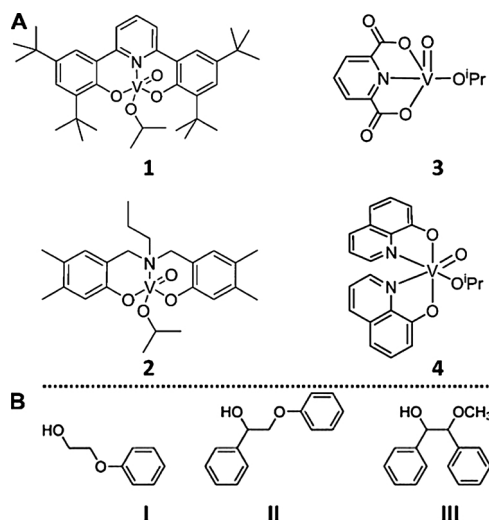

Fig. 10. (**A**) Oxovanadium complexes screened for the C−C bond cleavage reaction. (**B**) Simple lignin model compounds as substrates.

excellent selectivity for a wide range of model compounds which also include the phenolic functional group generally found in real lignin. The subsequent reductive C_β–O cleavage proceeded in the presence of excess HCOOH and DIPEA additives (Scheme 13). [93]

2.9. Selective C−O bond scission by CdS QDs

Very recently, this year Wu et al. has reported the successful utilization of colloidal cadmium sulfide quantum dots (CdS QDs) [94] for the selective degradation of lignin models as well as native lignin of woodmeal by solar energy-driven cleavage of the β−O−4 bond at room temperature (Fig. 9). This catalytic method being heterogeneous, helps to reuse the photocatalyst, colloidal CdS as shown in the Fig. 8c. In their study, the group has also investigated the selective degradation mechanism by employing different scavengers (hole, electron, and radical) and found that in the presence of these various scavengers, the
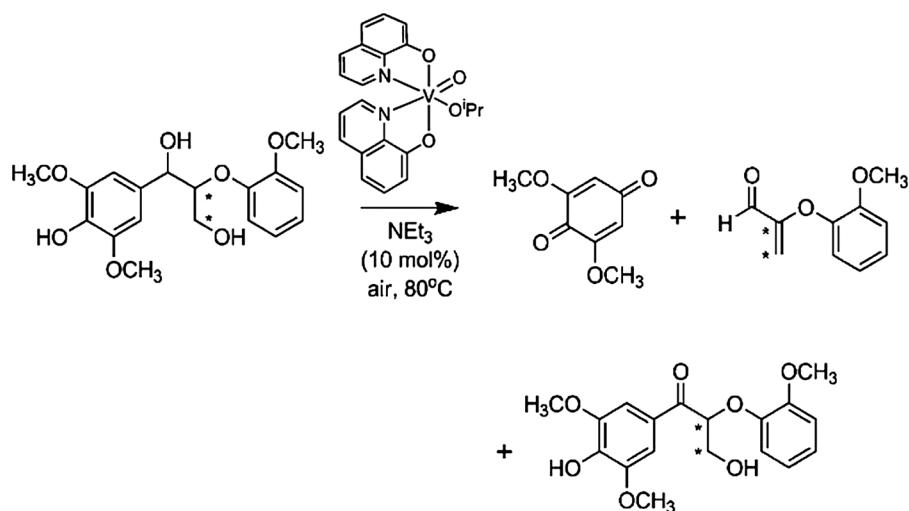
Scheme 15. Aerobic oxidative sp^{3}C$_\alpha$–sp^{2}C$_{aryl}$ bond cleavage of phenolic lignin model compound under the thermal condition catalyzed by complex **4**.
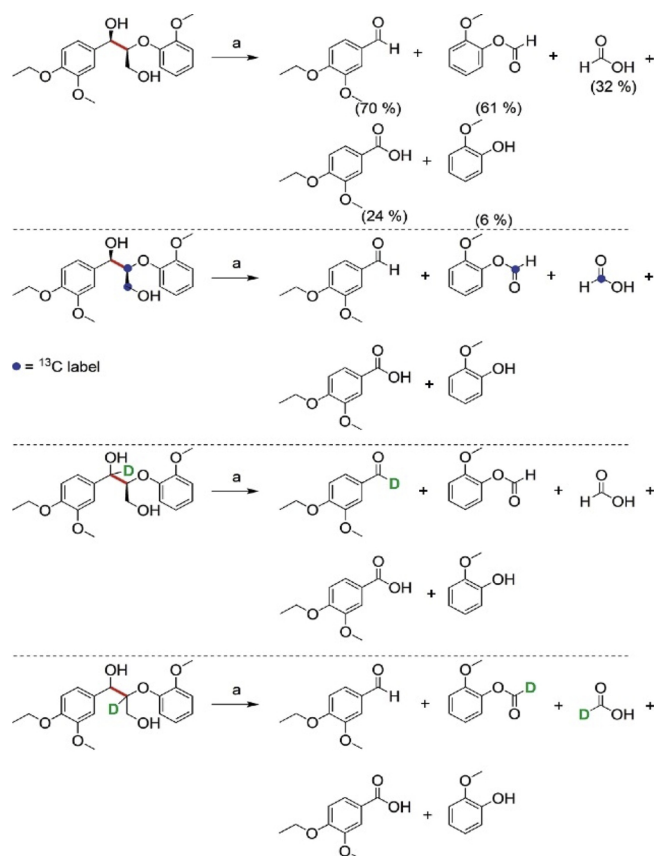
Scheme 16. Distribution of products from the photocatalytic C$_\alpha$–C$_\beta$ bond scission of lignin models with isotope lebeling.
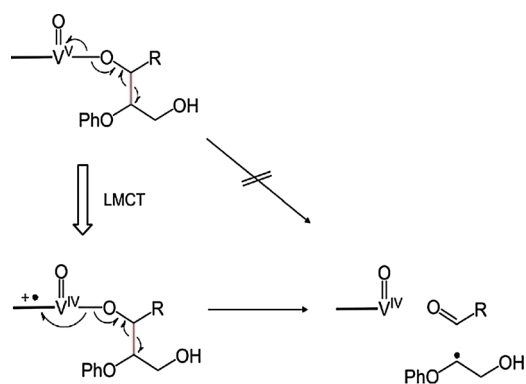

Fig. 11. LMCT-driven homolytic C–C bond cleavage. Reprinted with permission from Ref. [99]. Copyright 2015 Royal Society of chemistry (Chemical Science).

These studies revealed that in the degradation process effective charge separation occurs on the catalyst upon light irradiation, and the substrate lignin model or lignin generates a C$_\alpha$ radical intermediate by interacting with positive hole produced on catalyst upon light irradiation (Scheme 14). This fact was further confirmed by successful entrapment of the radical with a radical trapper, DIPPMPO (5-diisopropoxy-phosphoryl-5-methyl-1-pyrroline-*N*-oxide). Supported by the experimental evidences and the theoretical calculations they proposed the selective C$_\beta$–O bond scission mechanism of the β−O−4 linkage in lignin (Scheme 14).

3. Selective C–C bond scission

The bond dissociation energy (BDE) of the C$_\alpha$–C$_\beta$ bonds in β−O−4 lignin is generally higher compared to that of the C$_\beta$−O bonds. [95] Notably, the BDE of the C$_\alpha$–C$_\beta$ increases from 70.5 to 84.7 kcal/mol when the C$_\alpha$−OH is oxidized to the corresponding ketone functionality, as a result of which the C$_\alpha$−C$_\beta$ bond scission become more difficult. Whereas such oxidation decreases BDE of the C$_\beta$−O bond from 69.2 to 55.9 kcal/mol leading to the easier cleavage of the β−O−4 linkage. [84] Again, the groups surrounding the C$_\beta$−O bond of lignin models are sp^{3}C−aryl and a hydrogen atom which are connected with C$_\beta$ of C$_\beta$−O, while one aryl is connected with O of the C$_\beta$−O bond. Whereas, the groups surrounding the C$_\alpha$−C$_\beta$ bond are a hydroxyl and an aryl which are connected with C$_\alpha$ of C$_\alpha$−C$_\beta$, and −O−aryl, −CH$_2$OH are connected with C$_\beta$ of C$_\alpha$−C$_\beta$ bond. These surrounding groups clearly suggest that the C$_\alpha$−C$_\beta$ bond is more crowded over the C$_\beta$–O bond of lignin models

formation of the degradation products *via* the C$_\beta$–O bond cleavage of a model compound got remarkably reduced (< 10%), unlike the non-scavenging pathway yielding high amount of degradation products (> 90%) [94].
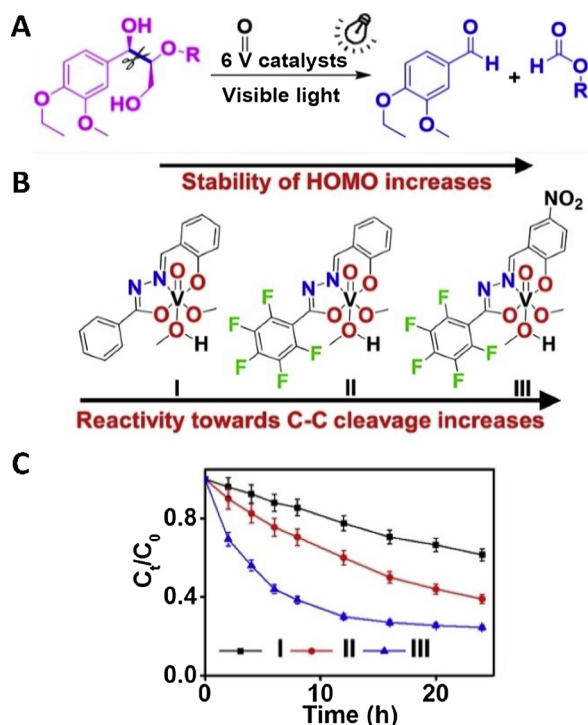
Fig. 12. (**A**) Schematic presentation of the selective C_α–C_β bonds of lignin models having the β−O−4 linkage by oxovanadium photocatalysts, (**B**) Structures of different vanadium based photocatalysts (I, II, III), and (**C**) Degradation kinetics of the lignin model (R = benzyl) with different photocatalysts (I, II and III). [100] Reprinted with permission from Ref. [100]. Copyright 2017 American Chemical Society (ACS Catalysis).
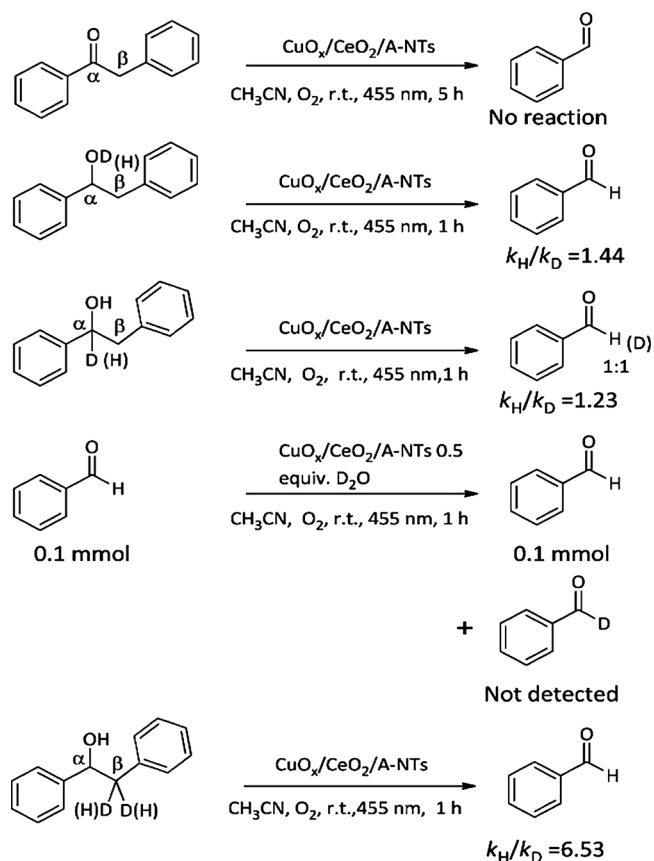
Scheme 17. Control Experiment and Kinetic Isotope Effects (KIEs).
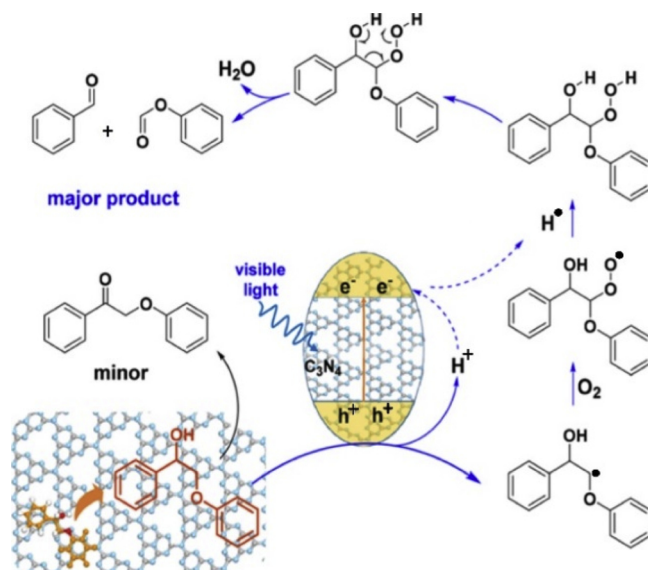
Scheme 18. Proposed C−C bond cleavage catalyzed by mpg-C_3N_4. Reprinted with permission from Ref. [102]. Copyright 2018 American Chemical Society.

or lignin. This over crowdedness of the C_α–C_β bond may act as the hindrance for the direct activation of the C_α–C_β bond in the selective bond scission. In fact, the presence of C_α–C_β bonds in the lignin structure makes it to be recalcitrant for its degradation. Again, the C−C single bond which is the most nonpolar bond present in the lignin, cannot easily be activated. Thus, in the literature, there are less references on the degradation of lignin models as well as native lignin *via* the C−C bond cleavage over the C_β–O bond cleavage.
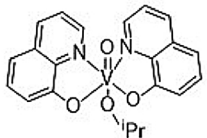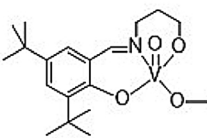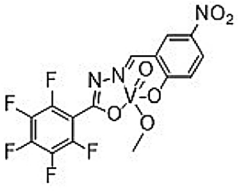
3.1. Selective C−C bond scission by V complex

The major work on C−C bond cleavage reaction by vanadium complexes was done by Hanson and his team. [96–98] A variety of oxovanadium complexes (Fig. 10A) have been screened for the C−C bond cleavage reaction of different substrates.

The group has conducted a series of experiments to evaluate the ability of the dipic vanadium complexes to catalyze oxidative C−C bond cleavage reaction. They observed that 10 mol% of complex catalyzed the aerobic oxidation of pinacol upon heating after 48 h. Vanadium complex **3** also proved to be a competent catalyst for the aerobic oxidation of simple lignin model compounds (Fig. 10B).

It was observed that generally, the substrates with backbone phenyl substituents were oxidized more readily and the order of reactivity for the simple lignin models found to be I < II < III. [54] Among these different oxovanadium complexes, although **4** showed high oxidation property for the benzylic alcoholic functionality, [97] when it was treated with the phenolic lignin model having the β−O−4 linkage, at 80 °C it catalyzed the sp^3C_α–sp^2C_{aryl} bond cleavage reaction and produced the degradation products (Scheme 15). [98] The distribution of the degradation products was further verified by the ^{13}C isotope lebeling study [98]. On the other hand, the non-phenolic lignin models did not undergo such type of degradation reaction rather the complex **4** did the benzylic alcohol (sp^3C_α−OH) oxidation to generate the corresponding ketone. Thus Hanson's catalyst **4** is found to be very specific for the phenolic lignin.

Recently, we have developed and reported a vanadium(V)-complex which can harvest solar light. We have successfully utilized the V^V-complex (Scheme 16) as photoredox catalyst to cleave the C_α–C_β bonds of lignin models having the β−O−4 linkage regioselectively under visible light irradiation at room temperature. [99] The photoreaction generated two valuable products, aryl aldehyde and aryl formate in moderate to high yields. The direct cleavage of the C_α–C_β bond

Table 4
Selective bond scission of lignin models under different reaction conditions.

Entry	Catalyst	Catalytic doses	Selective bond scission	Reaction conditions	Reaction Time (h)	conversion (%)	Ref.
1.		10 mol%	$sp^3C_\alpha-sp^2C_{Aryl}$	heating at 80 °C, in the presence of atmospheric air	48	> 95	98
2.		10 mol%	$sp^3C_\beta-O$	heating at 80 °C, in the presence of atmospheric air	24	95	41
3.	Pd/C	2.5 mol%	$sp^3C_\beta-O$	heating at 80 °C, HCOONH$_4$ (1 eqv.)	3	95	43
4.	Photocatalyst	10 mol%	$sp^3 (C_\alpha-C_\beta)$	room temperature, visible light irradiation (48 W white LED) in the presence of atmospheric air	24	76	100
5.	mpg-C$_3$N$_4$ Photocatalyst	10 mg / 0.05 mmol of substrate	$sp^3 (C_\alpha-C_\beta)$	room temperature, visible light irradiation (455 nm, 6 W LED), 1atm O$_2$	10	96	102
6.	i) CzCP100 Photocatalyst	2.5 mol%	benzylic oxidation	NHPI (20 mol%) room temperature, visible light irradiation (26 W CFL), O$_2$	24	90	93
	ii) CzCP33 Photocatalyst	2.5 mol%	$sp^3C_\beta-O$	room temperature, visible light irradiation (26 W CFL), DIPEA (5 eqv.), HCOOH(5 eqv.) O$_2$	24	90	93

in the lignin model was confirmed by ^{2}H and ^{13}C isotope labeling experiments, which revealed that there was no scrambling of benzylic hydrogen before or after the bond cleavage (Scheme 16). [99]

The mechanism of this unique bond scission reaction was investigated thoroughly by isotope lebeling study, intermediate trapping as well as theoretical calculations. Here, the TD-DFT calculation suggested that the excitation of the LMCT band in the alcohol-V^V-photocatalyst complex helped the hemolytic C$_\alpha$–C$_\beta$ bond cleavage (Fig. 11). The C-centered radical thus formed, reacts with molecular O$_2$ and finally get transformed into formate product. However, the substrates

with phenolic moiety did not allow the coordination of an aliphatic alcohol with vanadium. The DFT studies suggested a high activation barrier (> 30 kcal mol-1) for the C–C bond cleavage for such substrates.

Hence, a pre-process of natural lignin is essential to passivate all the phenolic groups prior to apply this approach for the C–C bond cleavage. We have further synthesized a library of modified V^V-photocatalysts by introducing strong electron-withdrawing groups such as NO$_2$ and F at the ligand with centres having the high spin density. That helps the HOMO energy level of the complex to be stabilized and the
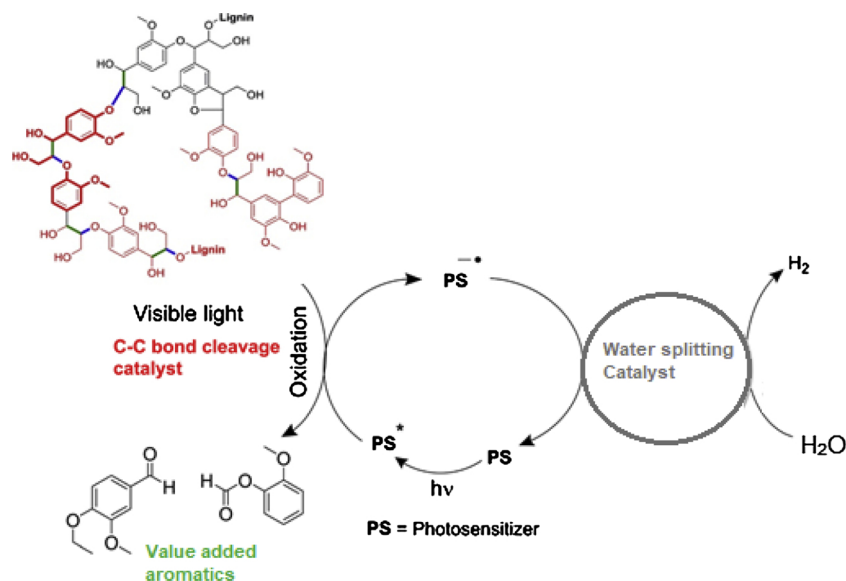
Scheme 19. Proposed catalytic duo for oxidative C−C bond cleavage and water splitting.

oxidation potential of the V^V photocatalyst is thus increased (Fig. 12) [100].

Mainly, the complex having one nitro group on the aryl hydrazone and pentafluoro substituents on the imidate moiety showed the greatest activity which was confirmed by the kinetics measurements, with the reaction rate up to seven times faster than the original complex. Our fundamental study on the LMCT induced C−C bond activation by vanadium photocatalysts is a unique and eco-friendly approach to harvest solar energy. This approach can potentially be employed in the valorization of (bio) macromolecules in the future.

3.2. Selective C−C bond scission by the CuOx/ceria/anatase composite

Soon after our report on C−C cleavage by V-photocatalyst, Wang and coworkers in 2017 also reported the C−C bond cleavage of β-1 models with 98% selectivity with a newly synthesized CuOx/ceria/ anatase composite used as a heterogeneous photocatalyst to accomplish the reaction under visible light irradiation (455 nm). [101]

The group carried out the mechanistic investigation by control experiments and kinetic isotope effect (KIE) experiments (Scheme 17). The experimental results suggested that the photogenerated holes abstracted the hydrogen from a benzylic carbon (C_β) to generate benzylic radical which in the presence of oxygen helped in the oxidative C−C bond scission to yield benzaldehyde as the product. Interestingly, in this approach there was no formation of the C_α−OH oxidation product (ketone) of the corresponding lignin model. The CuOx on ceria increases the surface oxygen vacancies and thus stimulates the C−C bond cleavage. The partial electronic density of states (PEDOS) calculation suggested that due to the shifting of the valence band edge of TiO_2 to higher energy, CuO_x on anatase nanotube prevented unwanted oxydehydrogenation reactions.

3.3. Selective C−C bond scission by mpg-C₃N₄

Very recently, Wang and co-workers have reported a new photocatalytic system based on mesoporous graphitic carbon nitride (mpg-C_3N_4) which upon visible light irradiation in the presence of molecular oxygen gave nearly full conversion and 91% selectivity of C_α−C_β bond cleavage of the lignin model having β−O−4 linkage. [102] The product were similar (benzaldehyde, phenyl formate, and benzoic acid) as we reported with vanadium photocatalysis. The high efficiency of the photocatalyst mpg-C_3N_4 was due to its large surface area and low

charge recombination supported by the low photoluminescence. The molecule activation and charge transfer process take place as the favorable π-π stacking interaction between the benzene rings and corrugated C_3N_4 surface. [102] The occurrence of this process is supported by the control experiments and also by the DFT calculations.

The mechanism proposed by the group (Scheme 18) suggests that the photogenerated holes abstract the hydrogen from C_β, most likely at the surface basic sites as suggested by the 2D $^1H-^1H$ DQ MAS (double quantum magic angle spinning) NMR spectroscopy. Then the binding of O_2 with the C_β-centered radical followed by the cleavage of $C_\alpha-C_\beta$, O−O yielded the aromatic aldehyde and phenyl formate as the major products.

By this approach the low yield of degradation products were reported for the lignin models having phenols groups that limits the protocol for the degradation of native lignin containing phenolic moiety. A comparative reactivity of certain catalytic systems for the selective bond scission of lignin models are summarized in Table 4.

4. Conclusions and perspectives

Wood biomass Lignin has been identified as a potential renewable feedstock for the production of valuable aromatic chemicals. However, the valorization of lignin is a challenging job, as it has a highly irregular and complex structure. Transition metal based catalysis has been exploited for lignin valorization which generally needs drastic reaction condition *e.g.* high temperature with excessive additives. However, photocatalysis overcomes some of the issues associated with the thermal catalytic processes by offering milder reaction conditions. A number of fascinating protocols have been recently developed to cleave both C_β−O and C_α−C_β bonds of lignin model systems selectively with good to excellent efficiency under homogeneous as well as heterogeneous photocatalytic conditions at normal room temperature. Conversely, it should be noted that the current developed techniques are having limitations to be applied industrially.

Hence, more ground breaking research works are necessary to find out the best catalytic methodology which will provide very high selectivity by activating C−C or C–O bond to break down the native lignin very efficiently, and thus producing less variety of aromatics with high yields of the products. Hence the catalytic system with very high turnover number may have the ultimate industrial application to disintegrate the non-food-wood biomass lignin to value added aromatic compounds. The oxidatively selective bond cleavage pathway may be

one of the highly important route as it may further offer the lignin to be used as the source of electrons (Scheme 19). Hence with suitable catalytic duo the released electrons from oxidative bond scission of native lignin can be utilized to drive water splitting reaction for hydrogen production.

Conflict of interest

Nothing declared.

Acknowledgements

References

[1] M.E. Himmel, S.-Y. Ding, D.K. Johnson, W.S. Adney, M.R. Nimlos, J.W. Brady, T.D. Foust, Science 315 (2007) 804–807.
[2] M.C.Y. Chang, Curr. Opin. Chem. Biol. 11 (2007) 677–684.
[3] A.M. Ruppert, K. Weinberg, R. Palkovits, Angew. Chem., Int. Ed. 51 (2012) 2564–2601.
[4] R. Rinaldi, R. Palkovits, F. Schueth, Angew. Chem., Int. Ed. 47 (2008) 8047–8050.
[5] W. Boerjan, J. Ralph, M. Baucher, Annu. Rev. Plant Biol. 54 (2003) 519–546.
[6] A.J. Ragauskas, G.T. Beckham, M.J. Biddy, R. Chandra, F. Chen, M.F. Davis, B.H. Davison, R.A. Dixon, P. Gilna, M. Keller, P. Langan, A.N. Naskar, J.N. Saddler, T.J. Tschaplinski, G.A. Tuskan, C.E. Wyman, Science 344 (2014) 1–10.
[7] S.K. Ritter, Chem. Eng. News 86 (2008) 15.
[8] G. Brunow, B. Kamm, P.R. Gruber, M. Kamm (Eds.), Biorefineries - Industrial Processes and Products, Wiley-VCH Verlag, Weinheim, Germany, 2006, p. 151 2.
[9] F.S. Chakar, A.J. Ragauskas, Ind. Crops Prod. 20 (2004) 131–141.
[10] J. Zakzeski, P.C.A. Bruijnincx, A.L. Jongerius, B.M. Weckhuysen, Chem. Rev. 110 (2010) 3552–3599.
[11] C.O. Tuck, E. Pérez, I.T. Horváth, R.A. Sheldon, M. Poliakof, Science 337 (2012) 695–699.
[12] P. Gallezot, Chem. Soc. Rev. 41 (2012) 1538–1558.
[13] M.Y. Balakshin, E.A. Capanema, H. Chang, T.Q. Hu (Ed.), Characterization of Lignocellulosic Materials, Blackwell, Oxford, U.K, 2008, p. 148.
[14] F.G. Calvo-Flores, J.A. Dobado, ChemSusChem 3 (2010) 1227–1235.
[15] J. Zhu, X. Pan Jr., R.S. Zalesny, Appl. Microbiol. Biotechnol. 87 (2010) 847–857.
[16] F.S. Chakar, A. Ragauskas, J. Ind. Crops Prod. 20 (2004) 131–141.
[17] R. Rinaldi, R. Jastrzebski, M.T. Clough, J. Ralph, M. Kennema, P.C. Bruijnincx, B.M. Weckhuysen, Angew. Chem. Int. Ed. 55 (2016) 8164–8215.
[18] A. Toledano, L. Serrano, A. Pineda, A.A. Romero, R. Luque, J. Labidi, Appl. Catal. B 145 (2014) 43–45.
[19] P. Gallezot, Catal. Today 121 (2007) 76–91.
[20] J. Cornella, C. Zarate, R. Martin, Chem. Soc. Rev. 43 (2014) 8081–8097.
[21] M. Tobisu, N. Chatani, Acc. Chem. Res. 48 (2015) 1717–1726.
[22] Z. Sun, B. Fridrich, A. de Santi, S. Elangovan, K. Barta, Chem. Rev. 118 (2018) 614–678.
[23] M.D. Kärkäs, B.S. Matsuura, T.M. Monos, G. Magallanes, C.R.J. Stephenson, Org. Biomol. Chem. 14 (2016) 1853–1914.
[24] J. Zhang, ChemSusChem 11 (2018) 3071–3080.
[25] J. Zhang, Green Energy Environ. 3 (2018) 328–334.
[26] G. Cahiez, A. Moyeux, Chem. Rev. 110 (2010) 1435–1462.
[27] A. Roglans, A. Pla-Quintana, M. Moreno-Mañas, Chem. Rev. 106 (2006) 4622–4643.
[28] G.A. Molander, B. Canturk, Angew. Chem., Int. Ed. 48 (2009) 9240–9261.
[29] G. Evano, N. Blanchard, M. Toumi, Chem. Rev. 108 (2008) 3054–3131.
[30] E. Geist, A. Kirschning, T. Schmidt, Nat. Prod. Rep. 31 (2014) 441–448.
[31] S. Dabral, J.G. Hernandez, P.C.J. Kamer, C. Bolm, ChemSusChem 10 (2017) 2707–2713.
[32] Y. Wang, Q. Wang, J. He, Y. Zhang, Green Chem. 19 (2017) 3135–3141.
[33] E. Wenkert, E.L. Michelotti, C.S. Swindell, J. Am. Chem. Soc. 101 (1979) 2246–2247.
[34] J.W. Dankwardt, Angew. Chem., Int. Ed. 43 (2004) 2428–2432.
[35] D.-G. Yu, B.-J. Li, Z.-J. Shi, Acc. Chem. Res. 43 (2010) 1486–1495.
[36] B.-J. Li, D.-G. Yu, C.-L. Sun, Z.-J. Shi, Chem. – Eur. J. 17 (2011) 1728–1759.
[37] B.M. Rosen, K.W. Quasdorf, D.A. Wilson, N. Zhang, A.-M. Resmerita, N.K. Garg, V. Percec, Chem. Rev. 111 (2011) 1346–1416.
[38] P. Álvarez-Bercedo, R. Martin, J. Am. Chem. Soc. 132 (2010) 17352–17353.
[39] A.G. Sergeev, J.F. Hartwig, Science 332 (2011) 439–443.
[40] A.G. Sergeev, J.D. Webb, J.F. Hartwig, J. Am. Chem. Soc. 134 (2012) 20226–20229.
[41] S. Son, F.D. Toste, Angew. Chem., Int. Ed. 49 (2010) 3791–3794.
[42] J.M.W. Chan, S. Bauer, H. Sorek, S. Sreekumar, K. Wang, F.D. Toste, ACS Catal. 3 (2013) 1369–1377.
[43] S. Sawadjoon, A. Lundstedt, J.S.M. Samec, ACS Catal. 3 (2013) 635–642.
[44] N. Yan, C. Zhao, P.J. Dyson, C. Wang, L.T. Liu, Y. Kou, ChemSusChem 1 (2008) 626–629.
[45] J.-Y. Kim, J. Park, U.-J. Kim, J.W. Choi, Energy Fuels 29 (2015) 5154–5163.
[46] J. Zakzeski, A.L. Jongerius, P.C. Bruijnincx, B.M. Weckhuysen, ChemSusChem 5 (2012) 1602–1609.
[47] J. Park, S. Oh, J.-Y. Kim, S.Y. Park, I.K. Song, J.W. Choi, RSC Adv. 6 (2016) 16917–16924.
[48] Q. Xia, Q. Cuan, X.-H. Liu, X.-Q. Gong, G.-Z. Lu, Y.-Q. Wang, Angew. Chem., Int. Ed. 53 (2014) 9755–9760.
[49] Y. Shao, Q. Xia, X. Liu, G. Lu, Y. Wang, ChemSusChem 8 (2015) 1761–1767.
[50] Q. Xia, Z. Chen, Y. Shao, X. Gong, H. Wang, X. Liu, S.F. Parker, X. Han, S. Yang, Y. Wang, Nat. Commun. 7 (2016) 11162.
[51] T. Okuhara, Chem. Rev. 102 (2002) 3641–3666.
[52] A. Sarkar, P. Pramanik, Microporous Mesoporous Mater. 117 (2009) 580–585.
[53] Y. Shao, Q. Xia, L. Dong, X. Liu, X. Han, S.F. Parker, Y. Cheng, L.L. Daemen, A.J.R.- Cuesta, S. Yang, Y. Wang, Nat. Commun. 8 (2017) 16104.
[54] W. Vermeiren, J.-P. Gilson, Top. Catal. 52 (2009) 1131–1161.
[55] L. Dong, L. Lin, X. Han, X. Si, X. Liu, Y. Guo, F. Lu, S. Rudic, S.F. Parker, S. Yang, Y. Wang, Chem. 5 (2019) 1–16.
[56] L. Donga, Y. Xin, X. Liu, Y. Guo, Y. Wang, C.-W. Pao, J.-L. Chen, Green Chem. 21 (2019) 3081–3090.
[57] J.O. Strüven, D. Meier, ACS Sustain. Chem. Eng. 4 (2016) 3712–3721.
[58] V.M. Roberts, R.T. Knapp, X. Li, J.A. Lercher, ChemCatChem 2 (2010) 1407–1410.
[59] Y.-B. Huang, L. Yan, M.-Y. Chen, Q.-X. Guo, Y. Fu, Green Chem. 17 (2015) 3010–3017.
[60] V. Roberts, S. Fendt, A.A. Lemonidou, X. Li, J.A. Lercher, Appl. Catal. B: Environ. 95 (2010) 71–77.
[61] L. Shuai, J. Luterbacher, ChemSusChem 9 (2016) 133–155.
[62] V. Roberts, V. Stein, T. Reiner, A. Lemonidou, X. Li, J.A. Lercher, Chem. Eur. J. 17 (2011) 5939–5948.
[63] B.M. Rosen, K.W. Quasdorf, D.A. Wilson, N. Zhang, A.-M. Resmerita, N.K. Garg, V. Percec, Chem. Rev. 111 (2010) 1346–1416.
[64] Y. Feng, H. Yin, A. Wang, W. Xue, J. Catal. 26 (2015) 26–37.
[65] Y. Wu, S. Cai, D. Wang, W. He, Y. Li, J. Am. Chem. Soc. 134 (2012) 8975–8981.
[66] D. Wang, Y. Li, Adv. Mater 23 (2011) 1044–1060.
[67] S. Cai, H. Duan, H. Rong, D. Wang, L. Li, W. He, Y. Li, ACS Catal. 3 (2013) 608–612.
[68] I. Nakamula, Y. Yamanoi, T. Imaoka, K. Yamamoto, H. Nishihara, Angew. Chem., Int. Ed. 123 (2011) 5952–5955.
[69] M. Sankar, N. Dimitratos, P.J. Miedziak, P.P. Wells, C.J. Kiely, G.J. Hutchings, Chem. Soc. Rev. 41 (2012) 8099–8139.
[70] C.R. Kumar, N. Anand, A. Kloekhorst, C. Cannilla, G. Bonura, F. Frusteri, K. Barta, H.J. Heeres, Green Chem. 17 (2015) 4921–4930.
[71] A. Narani, R.K. Chowdari, C. Cannilla, G. Bonura, F. Frusteri, H.J. Heeres, K. Barta, Green Chem. 17 (2015) 5046–5057.
[72] J. Zhang, H. Asakura, J. van Rijn, J. Yang, P. Duchesne, B. Zhang, X. Chen, P. Zhang, M. Saeys, N. Yan, Green Chem. 16 (2014) 2432–2437.
[73] J. Zhang, J. Teo, X. Chen, H. Asakura, T. Tanaka, K. Teramura, N. Yan, ACS Catal. 4 (2014) 1574–1583.
[74] J.-W. Zhang, Y. Cai, G.-P. Lu, C. Cai, Green Chem. 18 (2016) 6229–6235.
[75] X. Yu, J. Chen, T. Ren, RSC Adv. 4 (2014) 46427–46436.
[76] I. Klein, C. Marcum, H. Kenttamaa, M.M. Abu-Omar, Green Chem. 18 (2016) 2399–2405.
[77] J. Sun, A.M. Karim, H. Zhang, L. Kovarik, X.S. Li, A.J. Hensley, J.-S. McEwen, Y. Wang, J. Catal. 306 (2013) 47–57.
[78] Y. Zhai, C. Li, G. Xu, Y. Ma, X. Liu, Y. Zhang, Green Chem. 19 (2017) 1895–1903.
[79] A. Brandt, L. Chen, B.E. van Dongen, T. Welton, J.P. Hallett, Green Chem. 17 (2015) 5019–5034.
[80] Y.-X. An, N. Li, H. Wu, W.-Y. Lou, M.-H. Zong, ACS Sustainable Chem. Eng. 3 (2015) 2951–2958.
[81] J.-L. Wen, T.-Q. Yuan, S.-L. Sun, F. Xu, R.-C. Sun, Green Chem. 16 (2014) 181–190.
[82] J. Tian, J. Fu, L.A. Lucia, J. Wood Chem. Technol. 35 (2015) 280–290.
[83] A. Diop, K. Jradi, C. Daneault, D. Montplaisir, BioResources 10 (2015) 4933–4946.
[84] S. Kim, S.C. Chmely, M.R. Nimlos, Y.J. Bomble, T.D. Foust, R.S. Paton, G.T. Beckham, J. Phys. Chem. Lett. 2 (2011) 2846–2852.
[85] A. Rahimi, A. Azarpira, H. Kim, J. Ralph, S.S. Stahl, J. Am. Chem. Soc. 135 (2013) 6415–6418.
[86] A. Rahimi, A. Ulbrich, J.J. Coon, S.S. Stahl, Science 315 (2007) 804–807.
[87] C.S. Lancefield, O.S. Ojo, F. Tran, N.J. Westwood, Angew. Chem., Int. Ed. 54 (2015) 258–262.
[88] J.D. Nguyen, B.S. Matsuura, C.R.J. Stephenson, J. Am. Chem. Soc. 136 (2014) 1218–1221.
[89] M.D. Kärkäs, I. Bosque, B.S. Matsuura, C.R.J. Stephenson, Org. Lett. 18 (2016) 5166–5169.
[90] I. Bosque, G. Magallanes, M. Rigoulet, M.D. Kärkäs, C.R.J. Stephenson, ACS cent. Sci. 3 (2017) 621–628.
[91] X. Zhang, J. Zhang, ACS Catal. 5 (2015) 2250–2254.
[92] X. Zhang, J.Z. Lu, J. Zhang, Chem. Mater. 26 (2014) 4023–4029.
[93] J. Luo, X. Zhang, J. Lu, J. Zhang, ACS Catal. 7 (2017) 5062–5070.

[94] X. Wu, X. Fan, S. Xie, J. Lin, J. Cheng, Q. Zhang, L. Che, Y. Wang, Nat. Catal. 1 (2018) 772–780.

[95] R. Parthasarathi, R.A. Romero, A. Redondo, S. Gnanakaran, J. Phys. Chem. Lett. 2 (2011) 2660–2666.

[96] S.K. Hanson, R.T. Baker, J.C. Gordon, B.L. Scott, D.L. Thorn, Inorg. Chem. 49 (2010) 5611–5618.

[97] G. Zhang, B.L. Scott, R. Wu, P.L.A. Silks, S.K. Hanson, Inorg. Chem. 51 (2012) 7354–7361.

[98] S.K. Hanson, R. Wu, L.A.P. Silks, Angew. Chem. Int. Ed. 124 (2012) 3466–3469.

[99] S. Gazi, W.K. Hung Ng, R. Ganguly, A.M. Putra Moeljadi, H. Hirao, H.S. Soo, Chem. Sci. 6 (2015) 7130–7142.

[100] S. Gazi, M. Đokić, A.M.P. Moeljadi, R. Ganguly, H. Hirao, H.S. Soo, ACS Catal. 7 (2017) 4682–4691.

[101] T. Hou, N. Luo, H. Li, M. Heggen, J. Lu, Y. Wang, F. Wang, ACS Catal. 7 (2017) 3850–3859.

[102] H. Liu, H. Li, J. Lu, S. Zeng, M. Wang, N. Luo, S. Xu, F. Wang, ACS Catal. 8 (2018) 4761–4771.